POLITECNICO DI TORINO

Master of Science in Mechanical Engineering – Masters' thesis

Structural health monitoring of Adhesive joints using Optical fibres

Supervisors:
Prof. Davide Salvatore Paolino
Ing. Raffaele Ciardiello
Alberto Ciampaglia

Candidate:
Ubaid Jeelani Tugoo

The academic year 2022/2023

Table of Contents

Acknowledgement

I begin with all gratitude to Allah, the Most Gracious and Most Merciful, for blessing me with the strength to pursue and accomplish all the challenges put forth. Indeed, what Allah makes easier for us comes with paths unimaginable. Alhamdulilah.

When IK says, “Aap ne ghabrana nahi hai,” and when Goswami says, “Kuch Bhi!” both become relatable when you are studying at Politecnico di Torino.

I write this with undoubted gratitude and pleasure that I am finalizing my journey in this course. This has been one journey of remembrance with so many ups, lows, and lessons, the best of which has been that there is no replacement for hard work, perseverance, and dedication. I am filled with too much joy and happiness to take the time to thank each and every person who has been a part of this journey of mine. First of all, I want to thank my supervisors, **Professor Davide Salvatore Paolino**, **Professor Raffaele Ciardiello**, and my co-supervisor, **Ing. Mohammad Abbasi**, who made the difference in my way of looking at things and believed in me while challenging me with tasks that at first seemed impossible but with their valuable suggestions and guidance turned out to be exponential learnings. Their behaviour has been an amalgam of patience and teaching. Every other day with them has made me realize how every small detail is a path changer in experimentation, how the utmost care has to be taken in every phase of the process, and how the learning never stops. Their dedication to the field of composites goes without saying, but I will always look up to these guys to walk on the path with the passion and honesty they show. Words will never suffice to describe how great it has been to be with you all.

I would never have been able to do anything in life had my parents not been the support they have always been by believing in my unorthodox stances and having faith in my decisions without any questions. I am lucky to have them, and I pray to grow old with them. Whatever little I have been able to do or might do in the future, it’s all because of you people. Siblings are a joy, and so are mine. **Dr. Anjuman** and **Haris**, who are already doing the best in their paths, keep me motivated to do much more and better.

Then there has always been a part of me that reflects my friends and my people. They have always been my constants. Whether I have been in search of some emotional support, casual laughs, illogical discussions, or technical help, they have been there with some taunts, jokes, and unreasonable laughs. **Junaid, Saleem, Faizan, Danish, Anjum, Aieman, and Nousheen**—I love you guys.

My roommates here, who taught me the basic skill of life, cooking, deserve to be mentioned surely. Sufyan, Hamza, and Umer, you guys have been nothing less than brothers. Thank you.

Mentioning her at last because she deserves a special mention, I want to take the time to thank **Dr. Maviya** for being the best person I could have met. You have seen me at my worst, and you have been sure even when I have given up on myself. This journey would never have been possible without you, and this is no exaggeration. I have seen myself fail here, and this has been one of the firsts in my life until now, but even then, you kept motivating me. I would consider myself lucky to have kept on this journey till the end.

Abstract:

Due to an increase in the usage of composites in the world of engineering in the past few decades, a rise has been observed in research related to the joining processes, especially, between composite parts. This thesis is mainly focused on structural health monitoring (SHM) in composite single-lap joints (SLJ). ADEKIT A236/H6236 has been used as the polyurethane adhesive manufactured by the SIKA (CH) company, and the adherends were made of carbon fibre/epoxy prepreg woven, named XPREG XC130. The backface strain on SLJ was measured employing the optic fibres (LUNA ODISI-B). Additionally, dimensional parameters of the joints (overlap length and adherend thickness) have been varied, and consequently, the effect of these has been monitored in terms of loading conditions and strain magnitudes. Furthermore, the results obtained from the above methodology used to measure the backface strain showed that there is a point on the surface of the SLJ that records a zero strain up to the point where the damage starts occurring in the joint. Afterwards, this zero-strain point starts acquiring strain up to joint failure.

List of Figures

List of tables

Chapter 1: Introduction

The usage of metals in industrial setups has always been a convention, and its roots are so deep that one cannot think of an alternative, but the introduction of composite materials has not only brought about significant changes in various industries, but it has also transformed the way metals were being viewed as a material of choice. One significant challenge in adopting composite materials as a substitute for metals has been their strength and toughness. Nevertheless, researchers have made a ground-breaking discovery by introducing carbon fibre as a viable replacement for metals. Carbon fibres have not only evolved as a substitute in terms of strength (however directional) but also cover up for the light weighting solutions that are highly sought by the automobile, aerospace, and other heavy-duty industries.

When it comes to joining components at the interface, conventional mechanical tools such as nuts, bolts, and rivets have been widely used. However, the implementation of these tools comes with a set of challenges, including high costs, cumbersome processes, and time-consuming assembly lines when weighing the entire lifecycle of these elements. Moreover, these joints are prone to malfunctions, often failing due to issues like slippage, stress concentrations, rusting, and oxidation. As a result, supplementary maintenance costs are incurred not only for the joints themselves but also for the interconnected components.

To overcome these deficiencies, the industry is actively seeking options for joining techniques and solutions. One promising approach is adhesive bonding, which involves the use of materials such as epoxy and polyurethane. Adhesive bonding offers several benefits over traditional mechanical methods. It provides a more cost-effective and efficient assembly process, reducing both time and labour requirements. Besides, adhesive bonds distribute stress more evenly, resulting in improved joint performance and enhanced overall structural integrity. Additionally, adhesive bonding can offer resistance against rusting and oxidation, contributing to longer-lasting and more reliable joints.

By embracing adhesive bonding as an alternative technique for joining components, the industry aims to master the limitations associated with traditional mechanical tools, ultimately improving efficiency, reducing maintenance costs, and supplementing the overall reliability of interconnected components.

To ensure the performance and reliability of adhesive joints, a meticulous examination is necessary. This entails achieving comparable levels of strength to those offered by conventional joints. Consequently, experimental conditions need to be designed to assess the behaviour of these joints under various working conditions. Test setups involving point loads, 3-point bending, cyclic loading, and fatigue are habitually employed to assess the reliability of adhesive joints. This process of perceiving and analysing joint behaviour is known as "structural health monitoring." Talking about structural health monitoring, simple tools like strain gauges, which are commonly used in experimental setups, could be used. But here, experimentation is going to exploit the properties of optical fibres for monitoring purposes. The precedence of using optical fibres over strain gauges is that monitoring over longer lengths is pretty easy without having to use new sensors because theoretically any gage length could be used, the minimum of which is 0.65 mm in the setup. The primary objective here is the monitoring of distributed strain fields in the specimen, which is made of composite material and joined together using adhesives. The material used for composite manufacturing is primarily glass or carbon fibre. The task thus overcomes various spatial constraints in terms of accuracy and the number of measurement points on the given specimen. Knowledge concerning the handling of optical fibres is necessary, as it requires a high amount of care and sensitivity to prevent any damage or breakage owing to the brittle nature of the fibres.

The analysis is carried out using the LUNA-ODISI 6102, which is part of the ODISI 6000 series. The modern advancement in materials and systems has given rise to challenges in terms of monitoring and thus carving out the required results, and the above-mentioned fibre optic system overcomes these challenges in a much smoother and easy-to-go way. It provides one of the most precise and high-definition distributed temperature and strain sensing capabilities available in the market. It thus offers maximum visibility and insight into the changes in terms of loading and strains at any location of the specimens. The LUNA-ODISI 6102 operates based on the Rayleigh backscatter effect, which will be discussed in the topics following. The Rayleigh backscatter effect is achieved through the inclusion of intended density changes between the core and the cladding, which means composition fluctuations within the fibre core during the manufacturing process [1]. The optical fibres that are being used have been manufactured by Optokon and ThorLabs. The design of the specimen is least affected by the application of the optical fibres since they can be either attached to the surface or embedded within the composite. However, handling the fibres can be challenging because the primary material used for manufacturing fibre is glass, which is practically brittle. When the fibre gets

exposed after removing the jacket or the external protective coating, the user must implement caution to avoid damaging the fibres, which could render them useless.

In the field of structural health monitoring, there are diverse techniques available for measuring changing strains, and the use of optical fibres is one of the most advantageous. This thesis will address the critical issues typically encountered when working with optical fibres and their operating principles. The experiments conducted throughout this thesis will be discussed individually, covering some optimal approaches in terms of getting better results and also in terms of analysing them. Finally, a conclusion will be drawn, including thoughts on future research directions.

Chapter 2: Literature Review

2.1 - Structural health monitoring

In the literature, structural health monitoring (SHM) has been elucidated as the process of acquiring, validating, and analysing technical data to facilitate life-cycle management decisions for components and materials that are used or are intended to be used [2]. What is the damage? If, due to some changes in the material or geometric properties of a component or a system, there is a negative change in the functioning of the system, this can be referred to as "damage." Damage also encompasses changes in boundary conditions and connectivity. Proper monitoring of these changes is the foundation of structural health monitoring. There is always a specified type of damage that is being earmarked to be detected properly, this determines the architecture of the system employed for SHM [3]. There are a lot of highly effective non-destructive evaluation tools accessible for monitoring structural health, including a wide variety of local techniques.

For composite materials and structures, the monitoring and management of structural health are crucial. Structural health monitoring (SHM) is an emerging technology. This technique consolidates advanced sensor technologies with intelligent algorithms to estimate the condition of structures dynamically in real-time or on demand. SHM offers benefits in terms of safety and reliability, the performance is amplified, the monitoring is automated with no need for supervision, and the life cycle cost estimation is reduced. Now, due to high-end research in SHM technology, researchers have come up with techniques that are both propitious and autonomous and are available to detect and access the condition of the composite structure in real time without much lag or delay in producing results. The main agenda behind the use of this distinctly sensitive and accurate technique is to prevent or forecast damage, reduce stoppage time, and decrease maintenance costs, which could get exemplified if not detected in the proper time [4].

If discussion is done about industries dealing with automotive, aerospace, and wind energy, one of the main fields of consternation for them is weight reduction, but composites with high strength-to-weight and stiffness-to-weight ratios become an archetypal choice for use in these cases. The use of composite materials can result in significant weight savings, which can lead to improved fuel efficiency and reduced emissions in transportation applications. Additionally,

the use of composite materials can lead to improved performance in terms of stiffness, strength, and fatigue resistance [5]. Along with abundant practical advantages of composites, they enable the freedom to be customized. The basic building blocks of composites are fibres. The tailoring is done in terms of the type, size, and orientation of the fibres or different matrix materials. This results in a different set of properties exhibited by the final products thus obtained. Thus, for a particular application with some specified properties, designers get a free hand in creating parts and components from the materials of the given/required property class.

Components made of composites are useful in cyclic loading conditions, due to their enhanced resistance to fatigue. The selection of matrix material is the basis for increasing the fatigue resistance of composite materials. What adds to the selection of the material used for the matrix is the orientation of the fibres and their distribution inside the volume of the component.

Thus, the combination of all these properties—high strength, durability, customization, and fatigue resistance—makes composite materials a pragmatic option in industries for a wide scope of operations.

Effective non-destructive procedures must be used if composite structures are to be monitored for quality and integrity. While utilizing these methods for the detection of damage and faults, the structure's attributes and geometry are preserved. Using these methods also guarantees that the structure's behaviour and functionality are not jeopardized in any manner. These methods include thermography, optical fibre sensing, X-ray computed tomography, ultrasonic inspection, and acoustic emission monitoring, among others. These methods enable the early diagnosis of damage, which can assist avoid catastrophic failure and lower the expenses involved in the overall repair or replacement of the building.

To investigate the state of damage in modern materials, including composites and structural components used in industry, NDT&E methods like Acoustic Emission (AE), Acousto-Ultrasonics (AU), Ultrasonics (UT), Digital Image Correlation (DIC), and Infrared Thermography (IRT) can be used. These methods can also be used to track deformation and damage development over time and length scales, and are integral to SHM systems. These methods can provide information and data about parameters that are related to structural performance, such as displacements between two points of reference, strains over the length of a component in a chosen direction, and stresses. This information, when combined with

advanced post-processing tools, can help infer the current operational state and remaining life of the structure, which will thus provide solutions to prevent any untoward incident from occurring.

2.2 - Composite materials

Composites emerged as a novel class of materials that were about to be labelled as the future of engineering in the middle of the twentieth century. A composite is any material that can be made by using two or more different and distinct components in such a way that the demarcation of each in terms of its unique properties and boundaries is preserved [6]. The majority of such materials consist of two constituents, primarily: a matrix, and an inclusion or dispersed phase. The matrix typically has high ductility and low fracture strength. The properties of the composite material are determined by the constituents' geometry and distribution, particularly in the dispersed phase [7]. The main aim of composite materials is to blend the unique properties of each constituent in such a way that the final material overcomes the limitations of individual materials. Figure 1, shows a comparative study between composites and other conventional materials with respect to the mechanical properties exhibited. Thus, in the new structure created, the properties achieved are the ones not possible in any single metal or material.

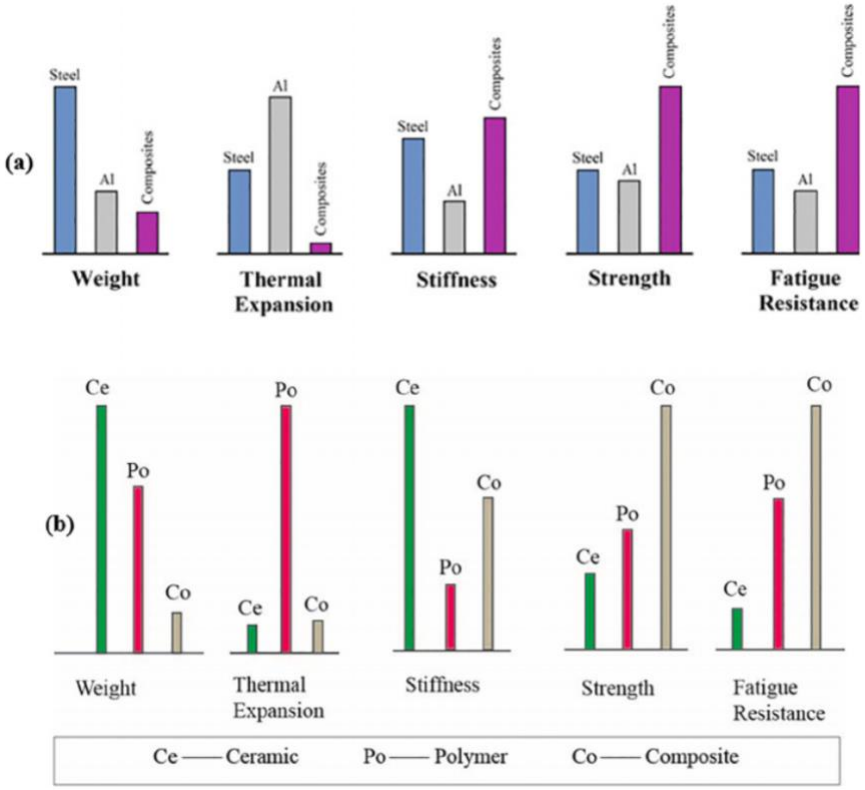

Figure 1 Comparison between mechanical characteristics of different materials[6]

A critical role is played by the dispersed phase in terms of achieving a symmetric load distribution inside the composite. For that, the process requires the resin to be evenly distributed in the die during the manufacturing process. Slight variations in the dispersion of the resin can significantly impact the properties of the resulting composite. For a change, once during experimentation on glass fibres, air bubbles were introduced inside the die, and the composite thus obtained had properties varying significantly from those without any air bubbles. To achieve the desired properties of a composite, it is crucial to carefully control the manufacturing process, ensuring the uniform distribution of the dispersed phase and the absence of any unintended elements. This attention to detail helps maintain the integrity and performance of the composite material.

2.2.1 - Types of composite materials

Since the properties of a composite material are predominantly determined by its constituents—the matrix and the dispersed phase—it is advantageous to have a range of materials that can be used as the matrix. This allows for further investigation and understanding of the mechanical properties of composite materials. Composites can be classified based on the type of matrix material used. This type of classification provides a more detailed and nuanced understanding of the mechanical properties of the composites obtained as such. And there are three types of matrix materials for the composite:

1. Polymer matrix composites (PMCs)

2. Ceramic matrix composites (CMCs)

3. Metal matrix composites (MMCs)

Polymer matrix composites have a long history if examined carefully. The development of composites, and as such, the introduction of metal and ceramic matrix composites, is rather a new addition to the vertical [8]. Initially, research was conducted on metallic and ceramic matrix composites. However, since the focus was primarily on continuous carbon and boron fibres, perfect, high-quality composites could not be achieved. But as the research interest in the field of fibres gained pace, accelerated results were obtained, and as a consequence, the

experimentation processes have now come to a point where the production of high-quality composites is easily possible [8]. Figure 2 shows the broad classification of the types of composites discussed.

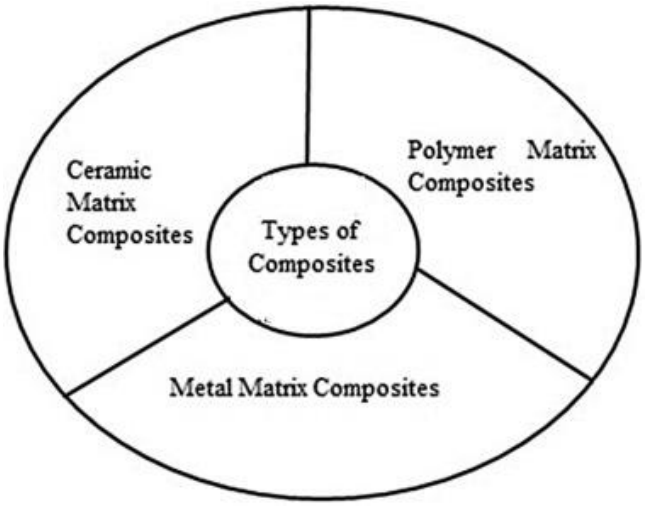

Figure 2 Types of composites [8]

Having discussed the type of matrix that could be used, it becomes somewhat obvious to expect a variety of types of resins. So, coming to the topic of resin classification, it can broadly be divided into two types.

1. **Thermoplastic resins:** as the name suggests, these resins somehow change their properties when exposed to changes in temperature. The first type of resin is thermoplastic resin, which is reusable after converting from the solid phase to the liquid phase by elevating temperatures and then curing it according to the requirements of the specimen or the test settings. The reusability of thermoplastics is a result of weak intermolecular forces between the polymer chains. Examples of thermoplastic resins include polyamides, poly(vinyl alcohol) (PVA), polyethylene, poly(tetrafluoroethylene), poly(vinyl chloride) (PVC), polypropylene, and poly(ether-ether ketone) (PEEK). However, when compared to thermosetting resins, their operating temperature range is smaller due to their high sensitivity to temperature. Additionally, the impregnation process with thermoplastic resins is highly difficult, which overshadows their other advantages, making them extremely challenging to use as the matrix for high-performance composites [9]. This must also be considered

because, after a certain number of times, the reusability starts to diminish due to damage in between the polymer chains.

2. **Thermosetting resins:** The second type of resin is thermosetting resin. The main difference between the two is that the thermoset resins are not reusable, and the process is thus not reversible. The reason behind this behaviour of thermosets is that the polymer chains in thermosetting polymers are interconnected by chemical reactions. If these resins are softened by heating, the chains break, which would mean no structural integrity of the resin as such, and thus it cannot be used in binding the composite together. Most of the reactions responsible for the formation of thermosetting resins are exothermic, so there is usually no requirement for external heat in the formation process. Thermosetting resins are of great interest and find wide usage in the fields of composites, coatings, adhesives, and electronic packaging owing to their excellent geometrical stability, resistance to chemical reactions, and outstanding thermal and mechanical properties, [10].

Resin transfer molding (RTM) and vacuum-assisted resin transfer molding (VARTM) are two usual techniques used for manufacturing composite components. To obtain a near-net shape of three-dimensional complex parts, the RTM process is used by employing good design practices, which leads to the production of cost-effective structural parts using low-cost tooling. However, the limitations of the process constrain the volume of production. VARTM, on the other hand, involves the use of a vacuum to assist with the resin transfer process, which allows for the manufacturing of larger and more complex parts [11]. Thermosetting resins have a highly cross-linked structure, which gives them better dimensional stability, high-temperature resistance, and resistance to solvents compared to thermoplastic resins. Thus, for manufacturing components with a higher life cycle, the properties of thermosets eclipse those of thermoplastics and make them the preferred choice in the world of composites [12].

The main types of materials used for the matrix are:

1. Glass fibres

2. Carbon fibres

3. Aramid fibres

Defining these types of fibres :

Glass fibre is a non-metallic inorganic material. It acts as insulation or resistance against heat and electricity. Additionally, it also demonstrates high tensile strength. Due to these properties, its usage in the conventional industrial setup is ample, and examples include transportation, petrochemicals, electronics, and aerospace. However, due to its relatively low modulus and heat resistance, the use of glass fibres is limited in certain applications.

For structural applications, carbon fibres are often preferred due to their high modulus, high strength, and low density. The composites made with a matrix and resins are directional, or anisotropic. So there will always be a different value for a certain property if the direction of measurement changes. In general, properties in the longitudinal direction (i.e. along the length of the fibres) are typically more useful as well as higher than properties in other directions.

Aramid fibres are known for their high tensile modulus and strength, which makes them suitable for use as reinforcement in advanced composites. For this purpose, aramids were the first organic fibres in use. The term "aramid" refers to fibres made of aromatic polyamide. In aramids, 85% of the concentration is that of the amide bonds (-CO-NH-) in connection with two aromatic rings directly. They too have a wide range of applications because of the strength properties they exhibit, but they are still not as good as those of carbon fibres [13]. Table 1 shows the different materials that can be used as fibres and their properties.

Table 1 Different materials used for fibres

Fibre Type	Density (g/cm^3)	Tensile strength (MPa)	Modulus of Elasticity (GPa)	Elongation at break (%)
Polypropylene	0.9-0.95	200-800	3.5-1.5	5-30
Polyethylene	0.92-0.96	80-600	5-117	3-100
Polyamide	1.14	750-1000	4.1-5.2	16-20
Polyvinyl alcohol	1.3	900-1800	20-42	6-8
Polyacrylonitrile	1.18	200-1000	2-19.5	2-3
Steel	7.84	350-3000	200-212	0.5-1
Carbon	1.4-1.7	2500-4000	230-380	0.5-1.8
Glass	2.5-2.6	1000-4000	70-80	1.5-3.5
Aramid	1.44-1.47	2300-3600	63-133	2-4.5

Dispersed phase

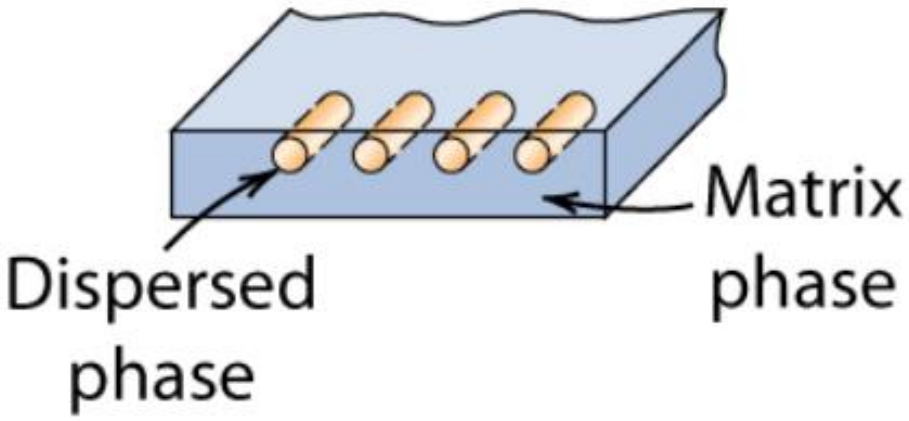

Figure 3 Dispersed and Matrix phase [14]

The "principle of combined action" states that the combination of two or more different materials with specific properties leads to the formation of composites. So to achieve a pre-defined set of properties that are not possible from the individual materials, this concept is applied. The application of composites in a wide array of industries, such as aircraft bodies,

brake shoes, and Formula One cars, is primarily because the weight of composites for the same volume of metals is very low, so there is an added advantage of weight reduction, whereas simultaneously the strength of composites is comparable to that of metals. Figure 3 shows a schematic representation of composite material. It consists of a continuous phase known as the matrix, which surrounds the dispersed phase. The dispersed phase also acts as support in the same way as iron rods or meshwork in the case of RCC. The basic principle is comparable and similar in both cases. The matrix protects the dispersed phase while allowing an even distribution of loading.

The properties of the dispersed phase, which could be in the form of fibres, particles, or flakes, greatly affect the properties of the composite material overall. The orientation, distribution, and volume fraction are some of the particular properties of the dispersed phase that can be varied, as a result of which they play a significant role in determining the overall mechanical and physical properties of the composite. For example, a high value of stiffness and strength is obtained in the composite material if the dispersed phase is well-oriented and has a high volume fraction. On the other hand, the composite material may not exhibit significant improvements in its mechanical properties compared to the matrix material alone if the dispersed phase is randomly oriented or has a low volume fraction.

The form in which the fibres would blend in the dispersed phase of the composites usually depends on the type of manufacturing process employed and the properties that are expected of the final composite. Non-woven fibres are usually randomly oriented. Composites made of non-woven fibres are isotropic. Woven fabrics, on the other hand, are arranged in a specific pattern that can provide anisotropic properties to the composite, depending on the orientation of the fibres. Bidimensional woven fabrics are typically used for two-dimensional components, while tri-dimensional woven fabrics are for three-dimensional components.

There are generally two particular directions of weaving fibres, perpendicular to each other: the warp and the weft. The warp direction is parallel to the production line of the fabric, while the weft direction is perpendicular with respect to the warp. There are several techniques for weaving the weft, giving rise to different patterns and characteristics in a composite. Different types of weaves, such as plain, twill, or satin weaves, will have different patterns and properties

[15]. **Error! Reference source not found.** shows different types of configurations that are available.

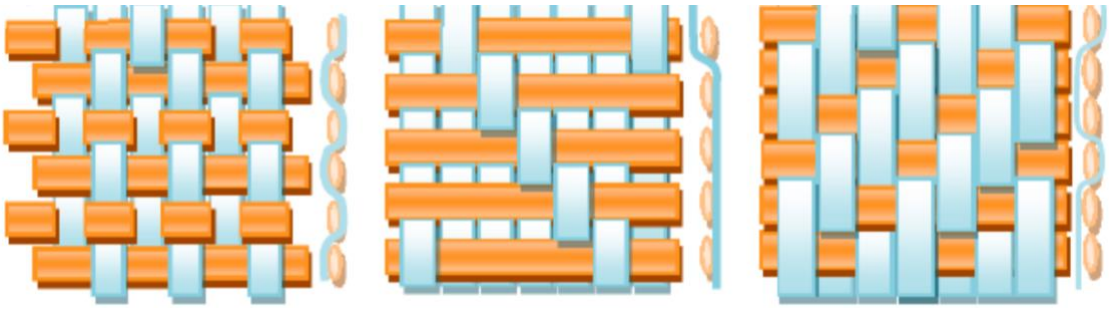

a) Plain weave. b) Satin weave. c) Twill weave [15]

Figure 4

Plain weave: It is the most simple and common type of weave design. It is the most inexpensive to construct because each weft goes alternately over and under one warp yarn.

Satin weave: In this, the pattern has one warp yarn over four or more weft yarns.

Twill weave: It is characterised by diagonal ridges formed by the yarns. Twill weaves are more closely woven.

To streamline the production of composite parts and samples, engineers have increasingly turned to the use of pre-pregs. These pre-pregs consist of fabrics that have been pre-impregnated with an optimal quantity of thermoset resin. The resin is partially cured, allowing for convenient handling, but it requires further curing to achieve the final cross-linking stage. This partially cured state is commonly known as the B-stage material. To ensure the proper curing process, it is essential to store and handle pre-pregs in a controlled environment. Cold temperatures are preferred, as heat can accelerate the curing process. By keeping the pre-pregs in a cold environment, the timing of the final curing can be managed. This ensures greater control and flexibility in the manufacturing process. The use of pre-pregs offers notable advantages in terms of reducing the time and effort required for composite production. It provides a convenient and efficient method for incorporating resin into the composite, ensuring consistent resin distribution and improved overall quality. The B-stage material characteristic of pre-pregs allows for easier handling and processing while still allowing for the necessary curing to achieve the desired material properties.

Inside the prepregs, there is continuous crosslinking happening between the resin and the curing agent. This process is initiated even before the actual curing process is started by the user. Thus, to avoid this automatic curing, the pre-pregs are stored in refrigerators, usually at around -18 ºC. By doing this, the cross-linking is limited [16]. Consequently, when the prepregs are taken out of the refrigeration environment, the available shelf life is very limited, and thus all the processing has to be finished in this available time [17].

Another aspect of prepregs is storage. Since it involves low temperatures, an increased burden of transportation and storage costs is seen; it has to be maintained at low temperatures even during transportation. Due to these reasons, the production costs of prepregs also increase. However, due to the storage requirement, the material performance of the prepregs in terms of compressive strength and modulus may decrease. Not only will the material performance be affected, but it will also affect the interlaminar strength [18]. Keeping the above-mentioned constraints in mind, the advantages of using prepregs also need to be considered. Using prepregs first reduces the processing time of the preparation of the samples, which in itself is a contrasting advantage to all the shortcomings. In addition, the shape of the final sample is uniform, and there is an equivalent thickness of the sample all over. This can also be considered in terms of surface quality, which is better than any other type of manufacturing technique used by far.

2.3 - Techniques for the production of composite polymer matrix

There are some consistent parameters on which any production technique depends. These include availability of labour, time, and technology. Process requirements and production costs vary as the technique changes. The quality and mechanical parameters of the final product depend on the method of production. The expectation from the product is to be of a near-net shape to encounter minimal post-processing.

Open-face moulding: the curing process takes place in an open environment, which means that the raw materials, i.e., resins and fibres are exposed to the environment. Different techniques can be used to carry out this process, such as hand layup, spray layup, or automated

layup, which can include tape layup or filament winding. It would be discussed in the course of this part.

Matched die moulding: is a reinforced plastic manufacturing process. There are two parts of the die, as in the case of moulding, which are close-fitting metals, matching male and female. Parts are formed when the two halves are connected, and then curing takes place with the effects of pressure, temperature, and time.

Pultrusion: it is an automated closed molding process used to manufacture fibre-reinforced polymer composites. In this process, fibre glass is pulled through a resin bath or impregnator. The process is carried on until the fibre becomes saturated. Then, to get the final product in a hardened shape, heated steel is used. The final product is a strong, lightweight fibre-reinforced polymer.

Discussing some of the main processes and techniques used:

- Hand lay-up process: the hand lay-up method is also called the wet lay-up method. It is one of the oldest methods used in industry. The main reason is the simplicity of this method. The thickness of the component to be produced is pre-defined, and for the same matrices, layers are stacked upon each other to reach the desired amount. All the plies are handled manually [19]. A big drawback of this method is its time consumption. An antiadhesive or wax is also used in the process over the mold surface where the resin and fibre are to be cured. This makes sure that the final product is easily separated from the mold and that no damage happens because of adhesion between the surfaces. A thin plastic sheet is applied at the top and bottom of the mold plates to ensure that the surface of the final product is smooth. Figure 5 shows a schematic diagram representing the hand lay-up process. The layers of woven reinforcement, which could be made of glass, carbon, or any other material, are cut to the required shapes and placed on the surface of the mold. The resin is mixed with other ingredients until the required specification is obtained and infused onto the surface of the reinforcement already positioned in the mold. For uniformity, a brush is used to spread this resin [20]. The curing process takes time as it is done at room temperature.

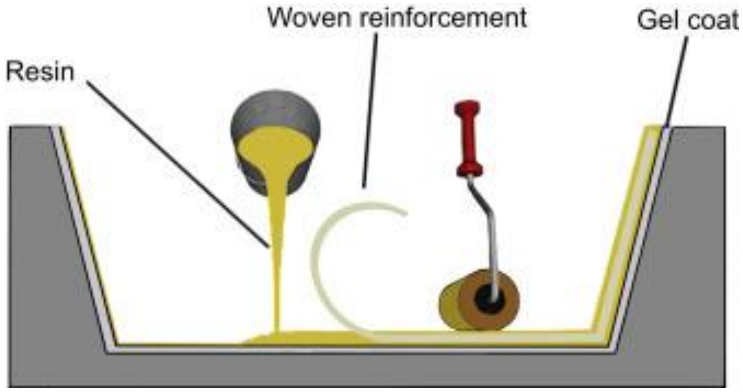

Figure 5 Hand layup[19]

- Spray layup process: similar to hand layup, an operator applies the composite material to single-sided tooling. An advantage of low-cost cooling is obtained in this procedure since the cooling is done at atmospheric temperature. Large parts can be produced using the spray layup process, but at an extended cycle time [21]. The main difference between hand layup and spray layup is that in the spray layup, a hand-held gun is used to spray the thermoset resin and the chopped fibres at the same time. It is thus faster because of a higher deposition rate. Figure 6 shows a schematic diagram representing the process.

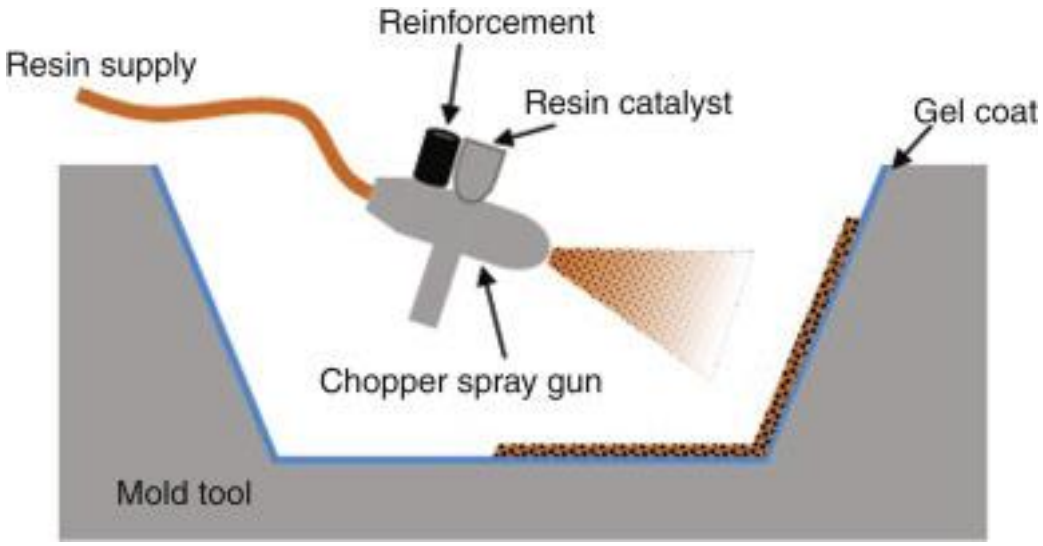

Figure 6 Spray layup[19]

- Vacuum bagging: Different types of structural components, such as carbon-epoxy, are fabricated using the Vacuum Bag Resin Infusion (VBRI) process and similar [22]. It is advantageous for an over hand layup and a spray layup as it provides a better surface finish and porosity to the component. The component is sealed to the tool or the glass plate using a plastic bag. The material is subjected to atmospheric pressure inside the bag by evacuating the air with the help of a vacuum pump. This process ensures a composite structure with improved properties [21]. The vacuum bag is also used for the curing of prepregs inside the oven. The oven accelerates the curing process.

Figure 7 shows various components that are part of the vacuum bagging process. Other components required in the vacuum bagging process are sealant tape, breather fabric, release film, and wax. The addition of these components makes the whole process complex and expensive. Also, the process requires using elevated temperatures in the oven to accelerate the curing process and also the vacuum pump, thus increasing the energy consumption.

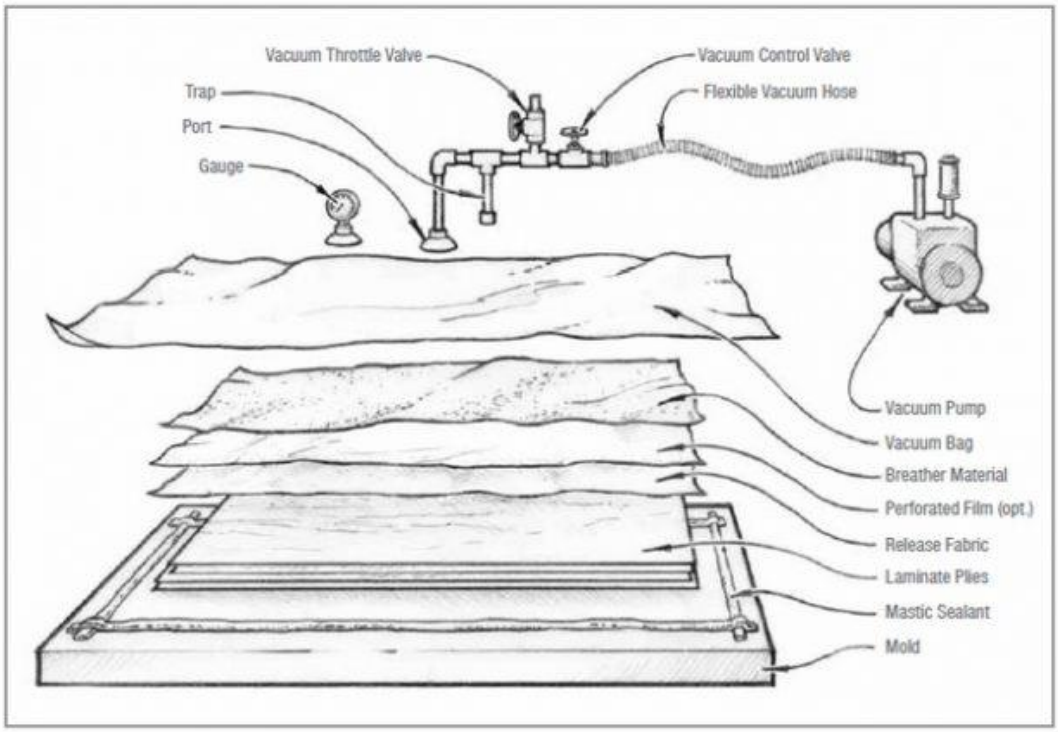

Figure 7 Vacuum Bagging[22]

- Resin infusion: is the process in which resin is inserted into the vacuum bag, which already has dry fibres whether woven or non-woven. It's almost similar to the vacuum bagging process, the only difference being that here an additional infusion of resin is done. In resin infusion, two openings are made into the vacuum bag: one for resin entry and one for the vacuum pump. A high fibre content composite is produced because of the vacuum, which draws the resin across and through the fabric. The resin is evenly distributed over the reinforcement. However, to get good impregnation, low-viscosity resin is used [21]. The curing generally takes place at room temperature, and as such, large tooling (and therefore parts) can be accommodated [21]. Figure 7 is a representative schematic.

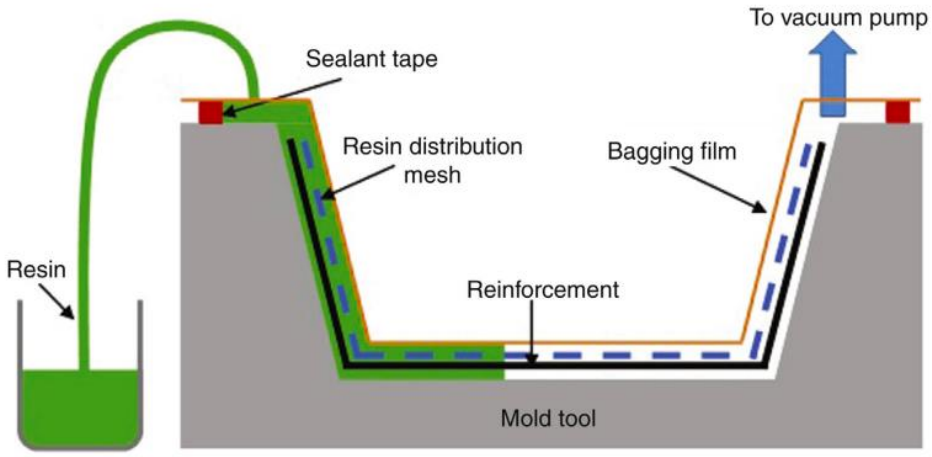

Figure 8 Resin Infusion[21]

- Resin Transfer Moulding (RTM): In this process, the male and female parts of the mold hold onto the fabrics, which take the shape of the mold. Then a passage of thermoset resin is allowed to flow through at an elevated pressure range of 2 to 20 bar. The process is dependent on some factors, which include, the pressure gradient in the tool, the viscosity of the resin, and the architecture and nature of the fabric, that is, its inherent permeability [21]. Once the fabric is completely wetted, the curing process of the composite starts. The curing starts at room temperature or higher temperatures. Due to the difference in temperatures, the time of curing also varies considerably, with a difference ranging from minutes to hours [21].

A schematic representing resin transfer moulding has been shown in Figure 9. Owing to the complexity of the shape of components, the RTM process can be time-consuming and inefficient. To overcome these constraints, some modifications have been made to the RTM process. If a vacuum is used for the RTM process, it's called Vacuum Assisted Resin Transfer Molding (VARTM), and if high pressure is used for resin transfer, it's called High-Pressure Resin Transfer Moulding (HPRTM) [21].

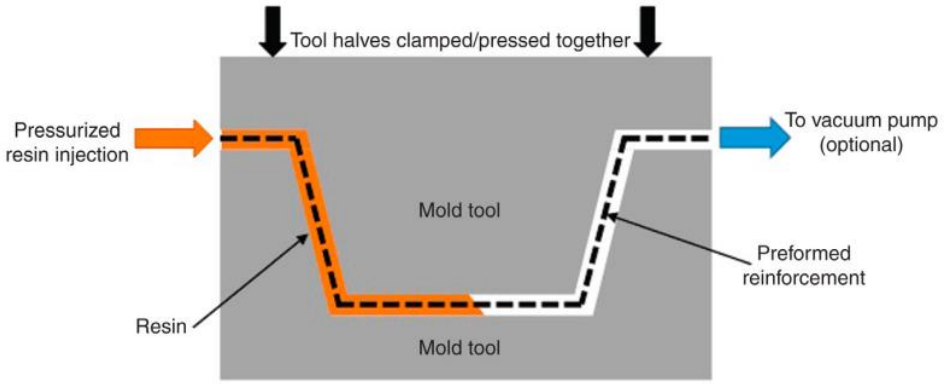

Figure 9 Resin Transfer Moulding [21]

- Compression Molding: In compression molding, the molding material is first placed in an open, heated mold cavity (female) or form (male) using a two-part mold system. The molding material is pre-heated so that it takes the shape of the mold [23]. A hydraulic press is used to distribute the mold material in the mold cavity. Compression molding is used to process bulk and sheet molding compounds (BMCs and SMCs), and subsequently cure while the heated mold tool is clamped shut [21]. Figure 10 shows a schematic of the compression molding process.

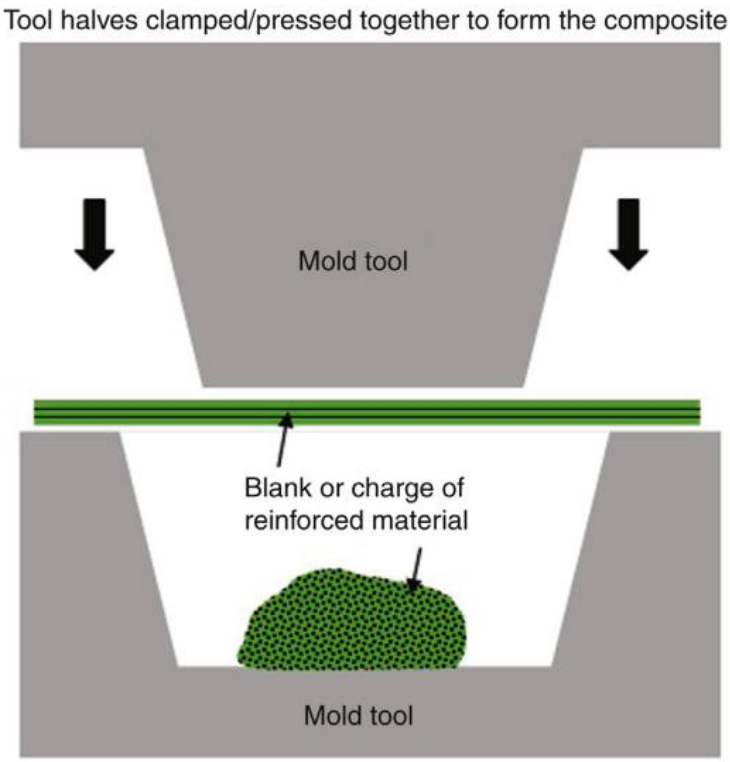

Figure 10 Compression molding [23]

- Injection molding: Injection molding works in some simple steps: there is a plastic melt that flows into the mold and takes the shape of the mold as the melt cools down; then the demold process is done. Injection molding makes parts in a discrete or discontinuous process [24]. Short fibre-reinforced thermoplastic is melted and homogenized by a rotating screw in a heated barrel. The direction of flow determines the direction of the fibres in the matrix.

- Extrusion: This process is similar to injection molding. In this process, plastic deformation of the material happens due to the application of force, causing that material to flow through an orifice or die. Water is used to cool the extrudate and solidify it. Then, it's either sectioned into lengths or rolled into coils [21]. High mechanical properties are not obtained from components manufactured by the extrusion process because of the use of short fibres.

- Pultrusion: This process is similar to extrusion. Here the material is pulled out of the die, while in extrusion the material is pushed out through the orifice. The resin-to-fibre

ratio is controlled by the use of die and pultrusion manufacturers' composites with a high fibre ratio [21].

2.4 - Adhesive bonding

The process of adhesive bonding involves using a non-metallic adhesive material placed between the faying surfaces of two or more parts to join them together through solidification or hardening [25]. Although the bonding created by adhesives shares similarities with brazing and soldering, the resulting bond is not metallurgical but rather chemical in nature. The components that are bonded together by the adhesive are referred to as adherends or substrates, which be composed of similar or dissimilar metals, composites, glass, plastic, or other substrate materials. Adhesive bonding used in the past was unreliable. Modern bonding materials have not only overcome conventional constraints but are also highly useful in equivalent load distribution, which produces joints with the lowest stress concentrations.

Adhesive bonding can be classified into two main types: structural and non-structural. Structural adhesive bonding involves bonding adherends under large stresses up to their yield point. On the other hand, non-structural adhesives are not designed to support significant loads but rather hold lightweight materials in place [26].

Discussion could also be done about thermoplastic and thermosetting adhesives, but they are almost similar to what has been mentioned in the previous section. Usually, being a thermoplastic or a thermoset is related more to the manufacturing process than the classification.

2.4.1 - Mechanical properties of composites bonded with adhesives

The mechanical properties that are exhibited by composites are dependent on the individual properties of the fibres and the resin and their interaction with each other. This interaction is dependent on the way the matrix layers are arranged, the type of production method used, and the technique of curing employed. The directional constraint of the matrix leads to anisotropy in the composites, and thus the properties vary tremendously as the direction is changed from longitudinal to transversal.

To prevent the loss of mechanical properties resulting from the use of conventional joining techniques of screws, bolts, nuts, and rivets, a lot of focus has been placed on the use of adhesive bonding. They protect the joints from stress concentrations and also allow for a uniform load distribution along the bond.

Damping properties and loading rate sensitivity are exhibited by polymer-based adhesives, which are used in structural applications, resulting in their high viscosity, especially at high temperatures [27] [28] or under water-cured and water-stored conditions [29].

The behaviour of an adhesive joint is governed by temperature variations as well as loading directions. Most of the adhesives used in structural applications exhibit viscoelastic-viscoplastic behaviour, especially at high-stress levels and high temperatures. The strength of the joint is highly affected by the redistribution of stresses and strains that occur in a joint during viscoelastic-viscoplastic deformation [28].

Studies have been done to obtain an analytical model for the mechanical behaviour of adhesive joints of different kinds. A study done on a lap joint to have a viscoelastic-viscoplastic stress analysis assumed the adhesive to exhibit a non-linear behaviour and the adherends modelled as two-dimensional substructures to behave in a linear elastic manner [28], only shear stresses were assumed to occur. Figure 11 shows how the variation of load occurs in the adhesive joint in a DCB at different time intervals.

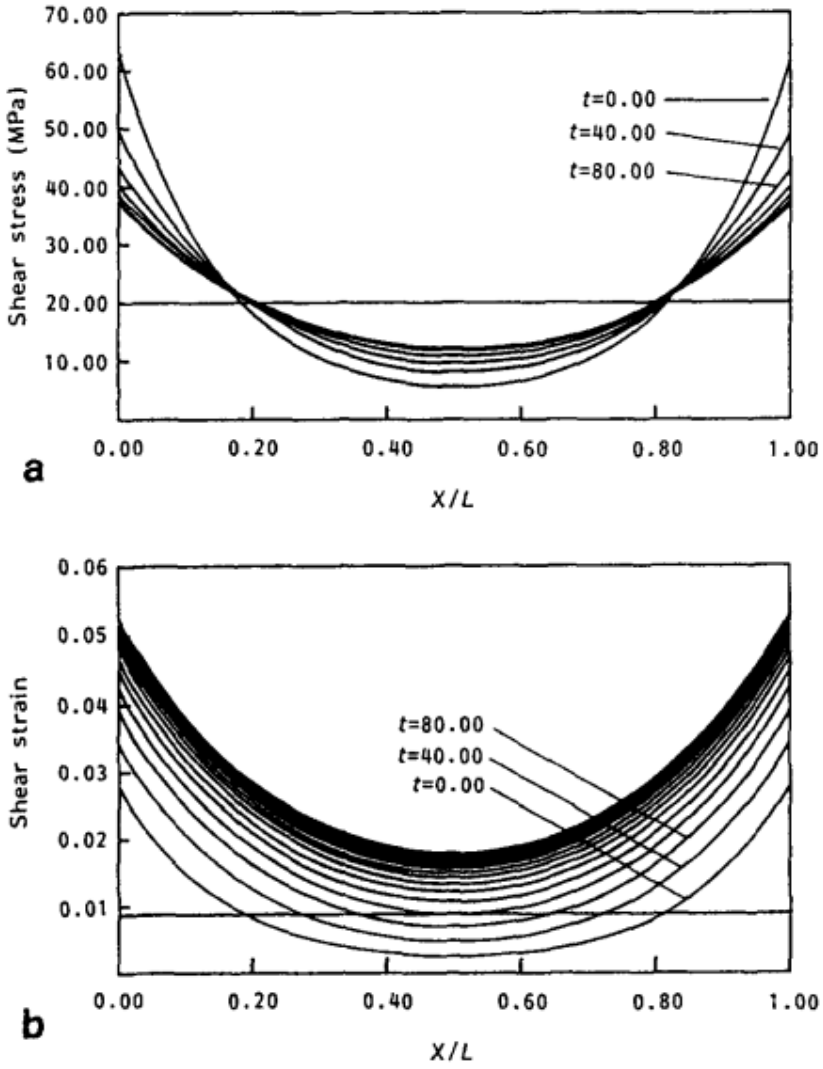

Figure 11 a) Shear stress behaviour. b) shear strain behaviour in DCB at different times [28]

Another type of test to check the behaviour of composites can be done using double cantilever beams (DCBs). Figure 12 is a schematic representative of DCB. The structure of DCB has a layer of adherend on the top and bottom and a layer of adhesive in between. The DCBs are chosen to check the strength of the joint in three opening modes: Mode I (peel), Mode II (in-plane shear), and Mode III (out-of-plane shear), as shown in Figure 13.

Figure 12. schematic of a Double Cantilever Beam

A well-established and standardized test on fibre-reinforced composites is the Mixed-Mode-Bending (MMB) test (viz. ASTM D6671, 2006), where a mode-mixity of mode I and II is achieved [30].

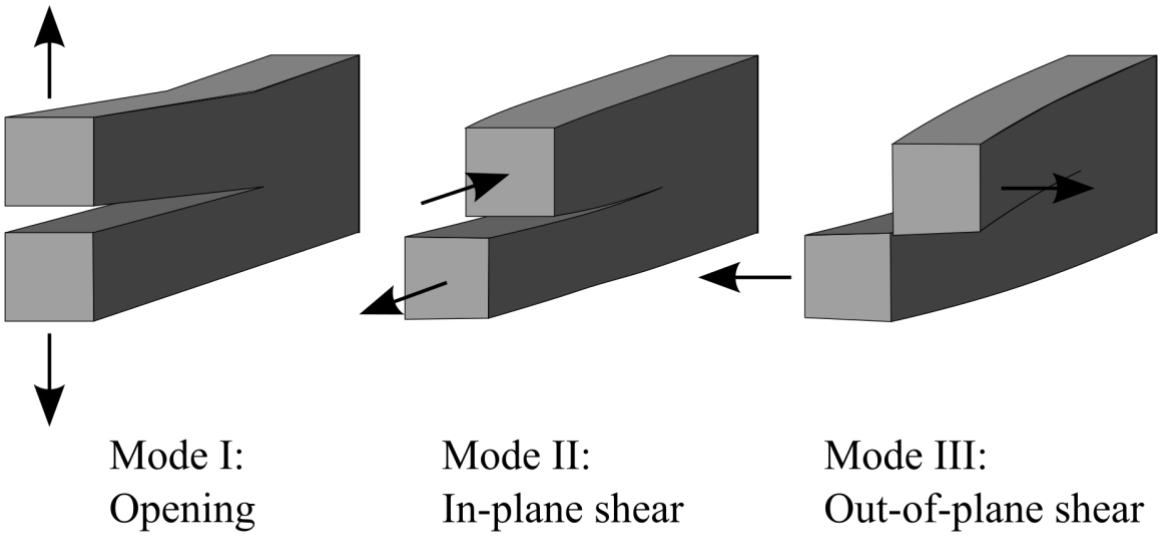

Figure 13 Bending in Mode I, Mode II and Mode III [30]

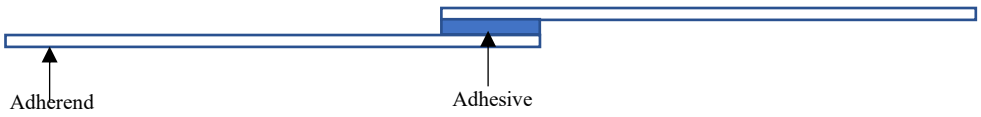

Figure 14 Representation of Single Lap Joint (SLJ)

Furthermore, studies have been done on the behaviour exhibited by lap joints joined using adhesives. The prime focus of this thesis is the behaviour exhibited by lap joints. Figure 14 is a schematic diagram of a single lap joint. The two adherends are joined using the adhesive in between. The variation in the dimensional features and the thickness of the adhesive layer or adherend show us the difference in the properties. Comprehensive studies have shown that there is an increase in the bending moment if there is an increase in the thickness of the adhesive. This changes the state of stress from a pure shear to a mixed shear with a peeling effect at the ends of the joint. Additionally, the treatment of the adherends near the surface of the joints also determines how the failure behaviour will finally be shown [adhesive failure or cohesive failure]. The surface treatment could mean anything from the cleaning agent coming

into use to the grade of the sandpaper for smoothening the surface [31]. Figure 15 shows the variation in shear loading as overlap length and adhesive thickness is varied.

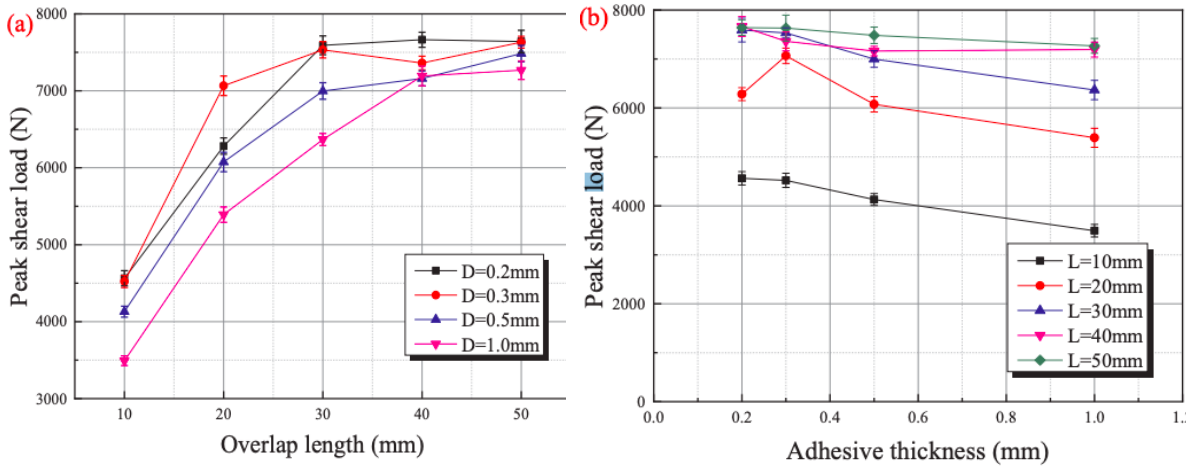

Figure 15 Peak shear load of the joints with different geometric parameters: (a) overlap length; (b) adhesive thickness [31]

An important role is played by the thickness of the adherend in determining the quality and strength of the joint. As there is an increase in the thickness of the adherend up to a certain limit while keeping the thickness of the adhesive constant, an increase in the strength of the joint can be seen [32].

2.5 - Strain measurement testing and analysis of adhesively bonded composites

Since composites are non-homogenous and anisotropic, it becomes challenging to maintain their structural integrity, making the detection and evaluation of damages even more difficult [33]. At different scales, defects and damages can occur, so it becomes very difficult to track and locate all the damage sites. This can result in complex damage mechanisms [34]. Thus, to maintain the structural integrity of the component and prevent any further increase in the damage already caused due to use, it is required to always have prevention against damage by testing, and thus reliance on non-destructive testing of the components is seen. This also ensures the safety of the structure and reduces overall maintenance costs.

Reviews are available on NDT methods used for composite research over different timelines, focusing on various aspects. Some of the particular studies done include those that concentrate on porosity in composite repairs, detection of damage due to cracks, determination of bond defects in laminates, thick-wall composites, sandwich structures, large-scale composites, smart structures, as well as inspection and structural health monitoring of composites. These studies are done especially for marine, wind turbine, and aerospace applications [33].

There are various categories of non-destructive tests and evaluation techniques, as shown in Figure 16:

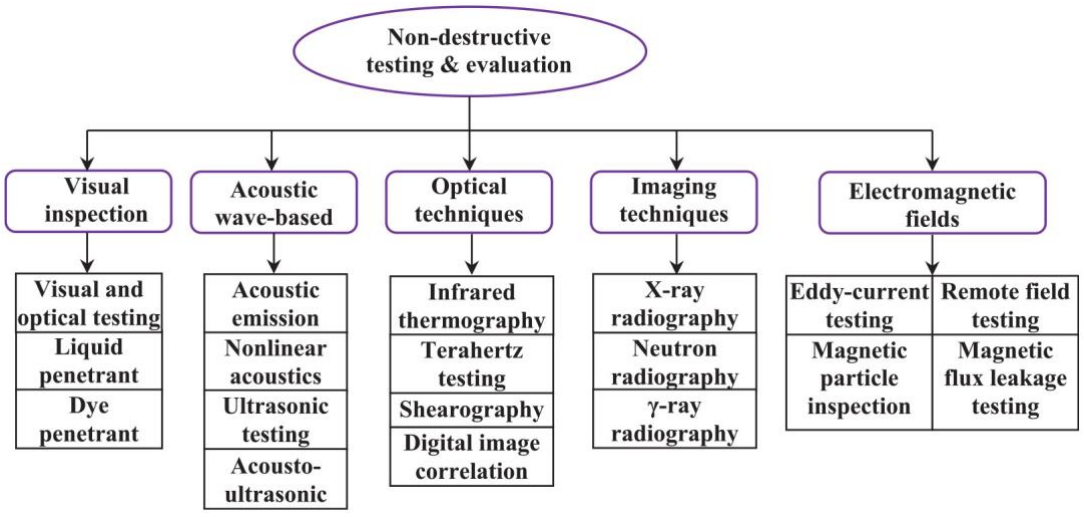

Figure 16 Classification of Non-destructive testing [33]

2.5.1 - Digital Image Correlation and Optical Sensors

Digital Image Correlation is an optical technique (non-destructive) in which tracking and image registration are done to accurately measure the changes in 2D and 3D images. This method can be utilized to track changes in the strain of a component. It is a widely used method in experimental and industrial applications of engineering. The DIC technique has the ability to provide both local and average data. Thus it outperforms the analysis obtained from strain gauges and extensometers. This method sets the standard for fine imaging and accuracy. A wide range of usage of the DIC is witnessed in micro- and nano-scale mechanical testing owing to its ease of use.

The basic idea is the comparison between a reference image and a deformed image. On the sample, a particular area is being monitored. This area is painted into speckle patterns using white and black background paints to make an even pixel distribution. Displacements and strains are measured by correlating the position of the blocks of these pixels [35]. Figure 17 is a schematic representation of the DIC setup.

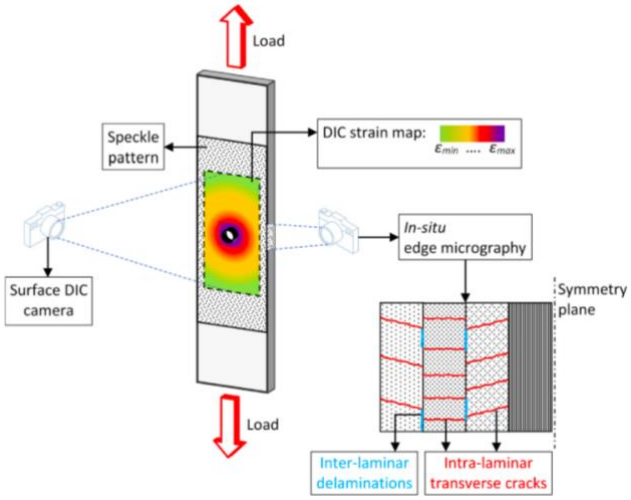

Figure 17 Schematic of DIC setup [36]

2.5.2 - Strain gauges

As the name suggests, strain gauges are devices used to measure strains or changes in strains in components. The strain gauges work on the principle of change in resistance due to mechanical stresses, thus, they can also be called electrical sensors. When stresses are applied to electrical conductors, a variation can be observed in the length of the sensor wires and the area of the cross-section, which results in a change in the resistance. So qualitatively, if the change in resistance is measured, it will give us the applied strains and stresses.

Apart from resistance strain gauges, researchers have also developed semiconductor strain gauges and high-temperature strain gauges. The semiconductor strain gauges are more sensitive and accurate than the resistance strain gauges. Care has to be taken in the circuit design. The introduction of these new types of strain gauges has increased the temperature limit of experimentation up to 1000ºC, which initially was at 400ºC [37].

1

$$R = \frac{\rho L}{A}$$

2

$$\frac{dR}{R} = \frac{(1+2\sigma)dL}{L} + \frac{d\rho}{\rho}$$

Where ρ is the resistivity of the wire, L is the length, A is the area of the cross-section, σ is the Poisson's ratio and R is the resistance of the wire.

The sensitivity of a strain gauge is determined by its gauge factor 'G'. It is defined, as the ratio of fractional change in resistance to the applied strain.[37]

3

$$G = \frac{\frac{dR}{R}}{\frac{dL}{L}}$$

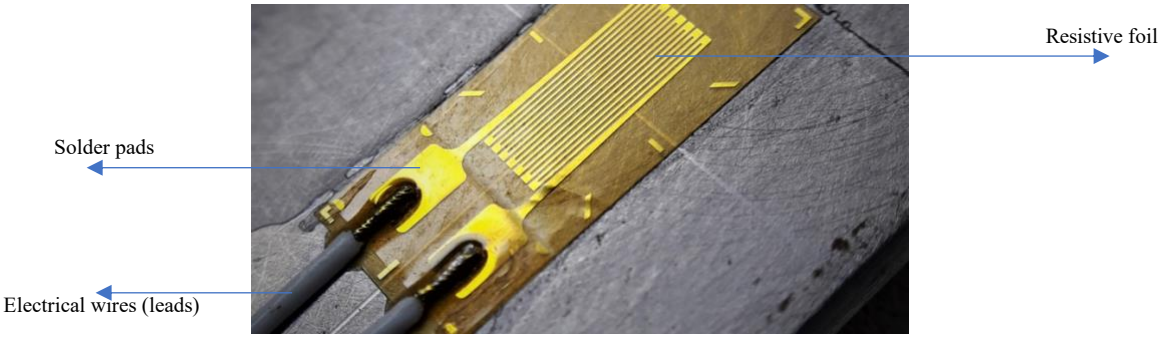

Figure 18 Resistance strain gauge[38]

Figure 18 shows a resistance strain gauge. Resistance strain gauges have limitations, rendering them suitable only for some particular cases. They can only be utilized in the given temperature range due to their temperature sensitivity. Additionally, resistance strain gauges are non-linear, which means they can function properly only up to their elastic limit.

Also, the strain gauges can be used for experimentation at a precise location. If analysis is required over the length of the component the cost of experimentation will increase, because of the number of strain gauges that have to be deployed for the completion of the task.

Having talked about the limitations, the point is that the applicability of these types of non-destructive testing methods in an industrial setup can become cumbersome. The results obtained are usually abstract and not tangible. Thus, to have a better method for testing and analysis, the focus shifted to the usage of optical fibres a few decades ago. They provide a solution to the shortcomings of other methods.

The optical fibres are more suitable for extreme environments such as corrosion and electromagnetic interference. Owing to the lightweight and small cross-sectional area of optical fibres, they can either be directly deployed on the surface to be tested or can also be embedded inside, thus increasing their extent of usage. Basically, they can be used to sense anything, be it a change in the liquid level, pressure, vibration strain, temperature, or electric field. While there are many different types of sensors designed to analyse signals from optical fibres, the process would mainly be talking about fibre Bragg grating sensors [39] and Rayleigh Backscattering.

2.5.3 - Optical fibres

Fibre optics, or optical fibres are long, thin strands of glass (the length can be considered to be infinite). They have a cross-section of the order of micrometres. These can be used in bundles or individually so as to analyse the signals transmitted through them over long distances. The fibre optics can also be considered a transmitting medium for the light signals, which are obtained at the receiving end and decoded at the other end using acquisition systems. The range of transmission can be over very long distances without any loss of signal.

Fibre optics works on the principle of refraction of light, or total internal reflection. The developments in the field of fibre optics have led to transfer speeds ranging from 45 Mb/s at the beginning to 100 TB/sec now and still evolving.

The optical fibres used in experimentation and industrial usage are brittle and thus require a safety coating to prevent breakage. Figure 19 shows the different parts or layers that an optical fibre is made of.

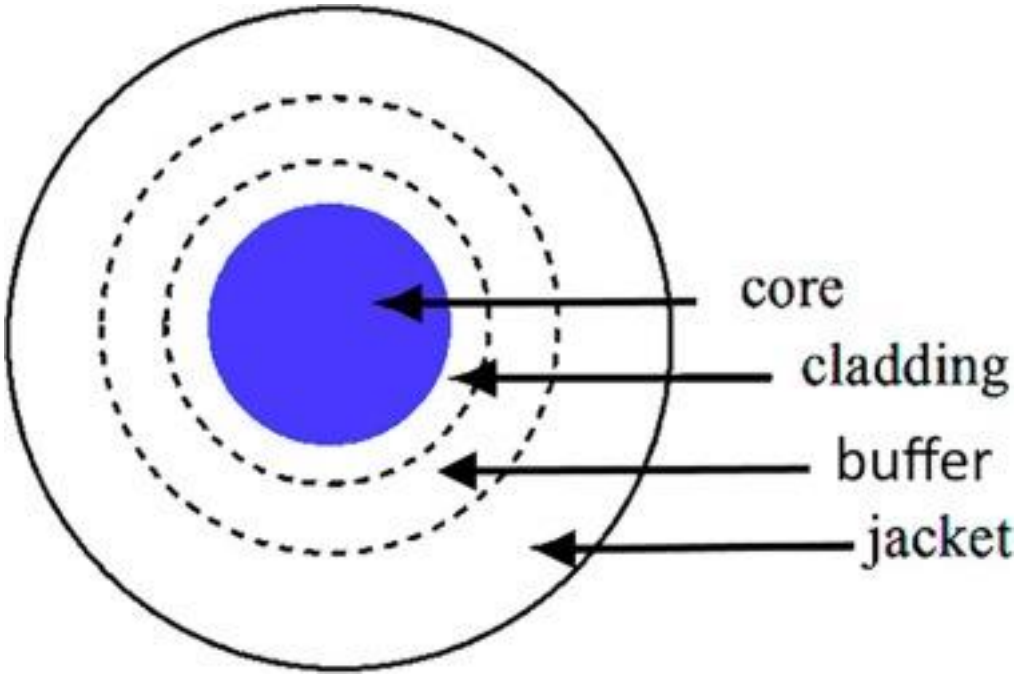

Figure 19 Layers in an Optical Fibre [40]

The phenomenon of total internal reflection occurs at the interface between the core and the cladding. The necessary condition for the occurrence of total internal reflection is that the incidence angle of light in the core should be greater than the critical angle. This condition ensures that the light is reflected back inside the core of the optical fibre and thus the propagation of the signal within the optical fibre happens. In addition to the critical angle, the refractive indices of the core and the cladding also play an important role in the amount or intensity of the light that is reflected back [40]. The total internal reflection phenomena are shown in different media in Figure 20:

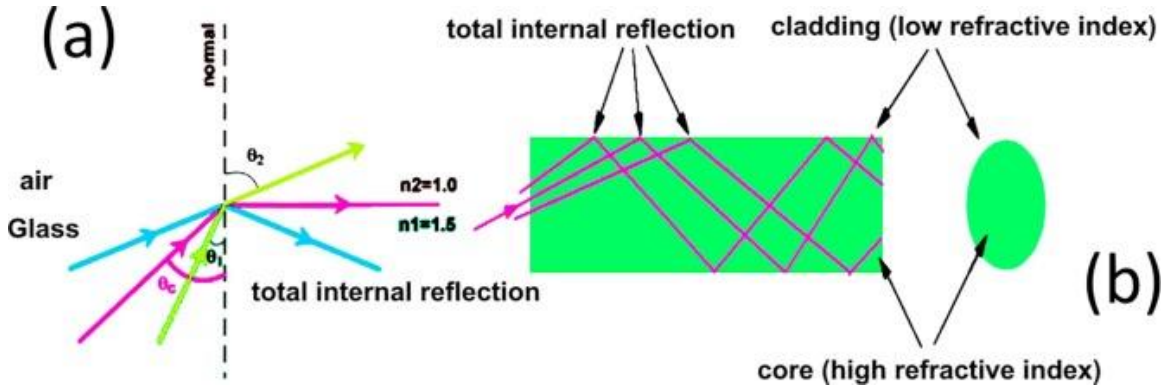

Figure 20 Total internal reflection (a) in air and glass medium, (b) in fibre structure which has two glass media with varying refractive indices [40]

Optical fibres are classified into different types depending on the applications they are being put into. The following are the aspects categorizing optical fibres:

1. Based on structure: Cylindrical, birefringent, planar or strip.

2. Based on modes of transfer: Single mode, multi-mode.

3. Based on refractive index profile: Single step, gradient index.

4. Based on dispersion: Natural, dispersion, dispersion shifted, reverse dispersion and dispersion winded fibre.

5. Based on signal processing ability: Passive data transmission, active amplifier.

6. Based on polarization: Classic, polarization preserving, and polarizing fibres.[40]

Explaining some of the mentioned types of fibres:

- Cylindrical optical fibres: Have a core, made of glass where the light passes through. The core is covered with cladding. The refractive index of the cladding is less than the core by around 0.005.

- Planar waveguide fibre: It has three layers of base, light guide, and coating, in the form of a rectangular block.

- Multi-mode fibre: Used for short-distance signal transfer. It has a large core diameter of around 50–62.6 um. Due to the large diameter of the core, the signals follow a varied number of routes, which results in the detection of waves at different times.

- Single mode transfer: These are more suitable for long-range signal transfer. The diameter of the core is small, of the order of 5-10 um [40].

The core of the optical fibre is usually made of glass or silica in its purest form. The main reason behind this is that the losses in silica are the lowest, thus making it the ideal choice for signal transfer and processing. For an optical fibre that needs to be used for highly sensitive operations, both the core and the cladding are made of glass. The inherent properties of the optical fibres such as low cost and ruggedness, make them suitable for usage in various applications.

2.6 - Manufacturing of Optical fibres

Manufacturing optical fibres is predominantly done by taking two processes into account: the crucible method and the vapour deposition method.

Double crucible method: In this method, there are two suitably joined concentric crucibles, and the core and cladding are obtained from molten glasses by drawing them through these crucibles. The crucibles are fed with highly purified glass powders with different refractive indices—the inner crucible for the core and the outer for the cladding. The melt obtained using an electric furnace, starts squeezing through the orifice. As the material starts cooling down,

the core starts diffusing into the cladding part, taking the final form of an optical fibre. As the fibre is drawn, thallium dopant is used, which has a high rate of diffusion into silica. Thallium dopant is used to maintain the refractive index. Figure 21 explains the working phenomenon of the double crucible method.

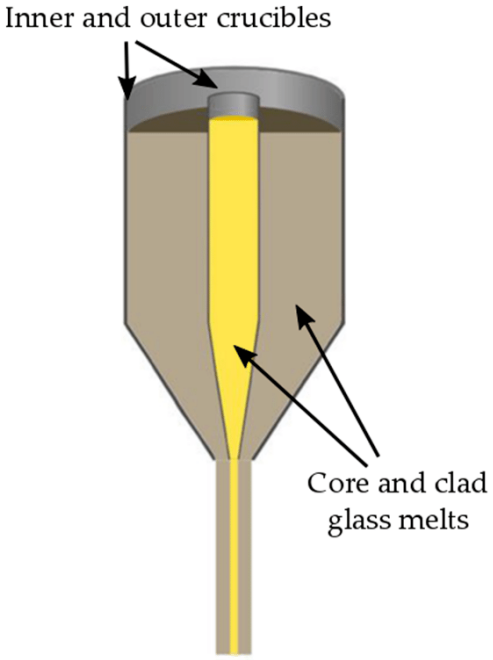

Figure 21 Schematic of Double Crucible method [41]

Modified chemical vapour deposition method: Used to manufacture high-performance optical fibres. After being subjected to fire, a layer-by-layer fusion of selected chemicals like germanium or phosphorus silicate is done on a glass tube. The glass tube, rotating on a lathe, mixes the chemicals. The flame is moved along the length of the burner, which causes the chemical reaction to take place, resulting in the deposition of the materials inside. As the deposition process finishes, the tube is collapsed into a pure form of silica that is drawn, checked, and coated for fibre fabrication. Figure 22 explains the process of the modified chemical vapor deposition method.

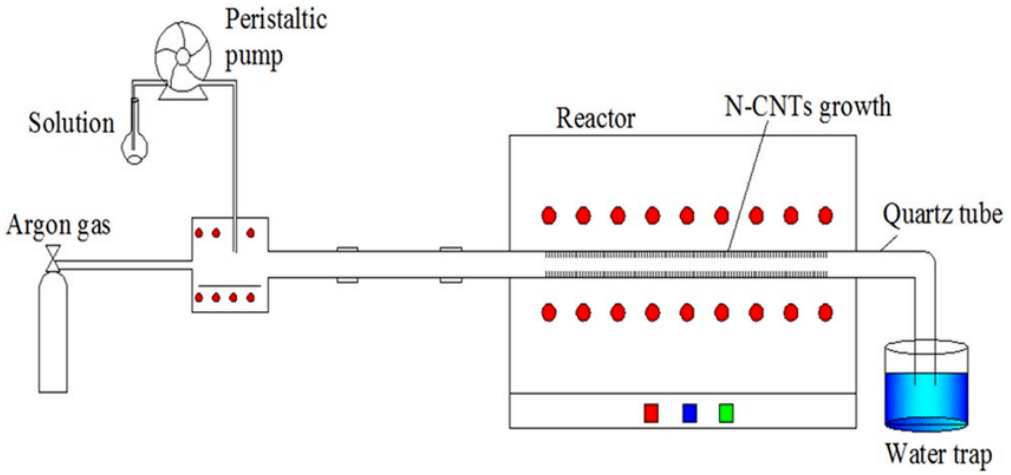

Figure 22 Schematic of Modified chemical vapor deposition method [42]

2.7 - Strain monitoring based on optical fibres

Fibres are getting used in the fields of remote sensing and telecommunications owing to their properties and accuracy of results. The properties range from their small size, easy mobility, and lack of use of electrical power. Additionally, the process can also sense the time delay as light passes along the fibres by using an optical time-domain reflectometer.

A fibre optic sensor uses optical fibres as sensing elements or as a transport agent. The signals travel from a remote location to the sensor, where the signal can be interpreted or demodulated. Sensors using optical fibres as sensing elements are called intrinsic sensors, while those using them as relaying agents are called extrinsic sensors.

Fibre optic sensors are used in sensing quantities like temperature, pressure, strain, stress, displacement, rotation, concentration of chemicals, et al. Taking these things into consideration, and discussing some of the optical sensors used:

2.7.1 - Fibre Bragg grating sensors

In fibre Bragg grating, along the length of the fibre, the refractive index goes through periodic perturbations, due to the intense optical interference pattern inside the core of the optical fibre. A narrow bandwidth of the incident light is reflected by the perturbations inside the fibre. The strongest of those occurs at Bragg wavelength λ_B which is given by:

$$\lambda B = 2 * \eta eff * \Lambda$$

Where η_{eff} is the modal index and Λ is the grating period. So there are in-phase fronts present after every λ_B distance. Any change in the pressure, strain or temperature which might change the modal index or the grating period will change the Bragg wavelength too [43].

It is a type of optical fibre sensor that encompasses almost all the advantages. Its attributes include low loss relative to fibre length, a signal that does not vary due to interference with electromagnetic or radio waves, accuracy in hazardous and extreme environments, low weight, high sensitivity, and reliability. Additionally, absolute values of measurement from FBGs can be used without the need for referencing.

Since the FBG sensors are wavelength-encoded, this is advantageous to the user. As a particular set of Bragg wavelengths is selected, each part or array of the sensor will register a change along its length while neglecting any changes from adjacent transducers or the transducers at a distance.

The effective refractive index gets shifted, which shifts the Bragg wavelength when there is any change or shift in strain.

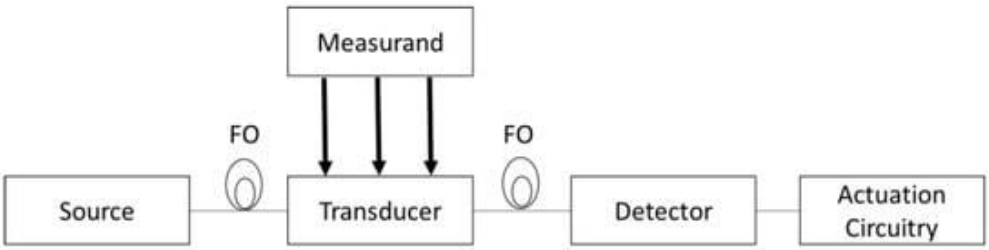

Figure 23 Fibre optic sensor simplified architecture [44]

Figure 23 explains briefly the architecture of a fibre optic sensor. It consists of an optical source used for the excitation of the transducer using optical fibre (FO). If there is any discrepancy in the measurand, the transducer converts the signal from the measurand into a signal with different features. Then the detector is used to analyse the modified signal, which is then processed using actuation circuitry.

Strain changes can be analysed using distributed sensing along the whole length of the component under investigation.

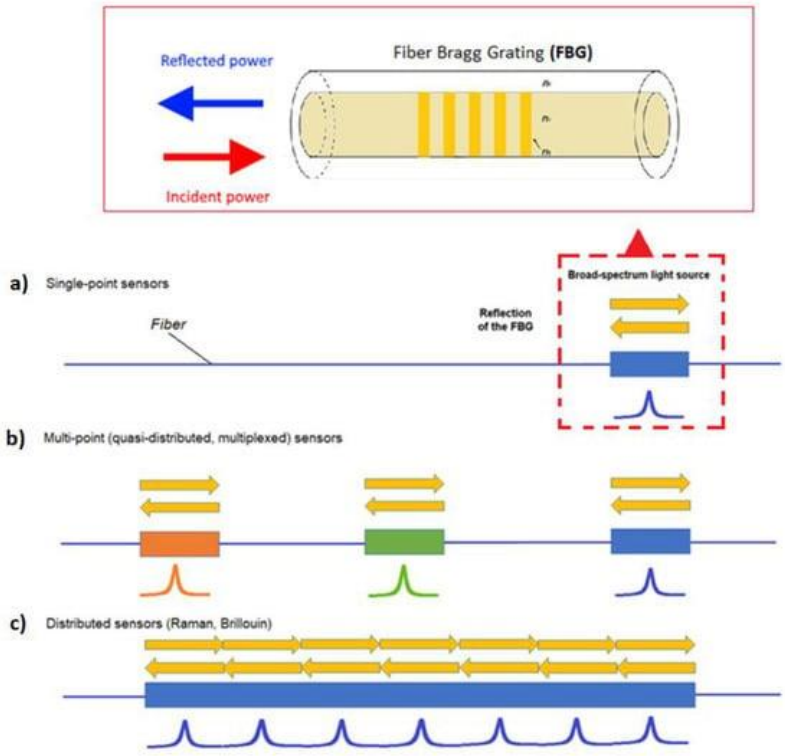

Figure 24 Fibre-optic strain sensing categories: single-point sensors, including (a) FBG sensors, (b) quasi distribute (multiplexed), and (c) distributed sensors[44]

Owing to the discontinuity at layer interfaces, some of the light gets reflected. This is due to discontinuity at the layer interfaces, where some parts get reflected while the remaining parts pass over. Thus, the beam contains two components travelling in opposite directions, giving rise to a coupling between the incident and the reflected light. And at some particular wavelengths, the Bragg condition is satisfied, this has been shown in Figure 24 for different types of sensors. These wavelengths are defined by the grating parameters [44].

Some additional advantages of FBG sensors can be summarised as direct measurement compared to conventional electric sensors; exhibiting a linear response to the measurements of strain or pressure; being electrically passive; being able to be used over long distances without loss in the signal; and the fact that each channel can measure dozens of sensors. Consequently, there are some disadvantages too, which can include sensitivity towards the thermal

environment, and the demodulation of wavelength shift being difficult. Also, if the process asks to discriminate the wavelength shift due to temperature and strain, it becomes quite a tedious job.

Being discrete in their functioning, the FBGs pose the imminent disadvantage of monitoring strains only locally, while the requirement is to monitor global behaviour. Owing to this constraint, the focus must be shifted to distributed sensors. Distributed sensors can be used in large-scale structures, such as high-rise buildings. Additionally, in these types of applications, the number of point sensors and the circuitry required for them might increase exponentially, which will increase the cost of installation and maintenance. Also, as seen in further studies, in the case of discrete sensors, the location of damage cannot be pointed out accurately as there is always some margin of error, which can be removed using distributed sensors [45]. Figure 25 shows a schematic installation pattern for point sensors and distributed sensors.

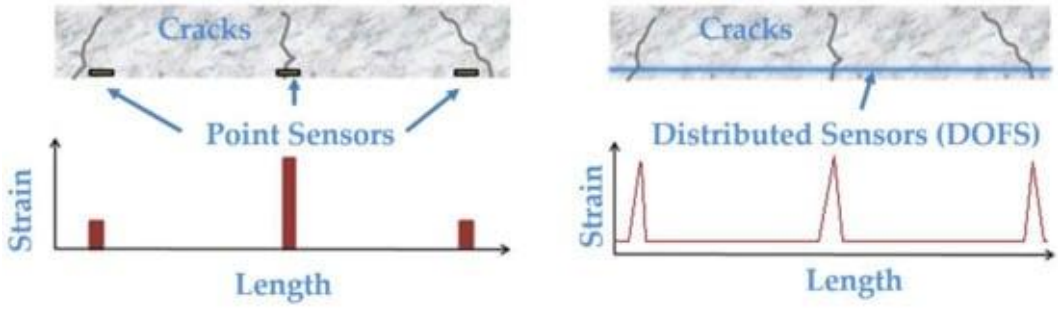

Figure 25 Strain detection using discrete and distributed sensors [45]

2.7.2 - The Optical Backscatter Reflectometry (OBR)

Optical Backscatter Reflectometry uses high spatial-resolution optical fibres to measure Rayleigh backscatter using swept-wavelength interferometry (SWI) as a function of the length of the optical fibres. The local Rayleigh backscatter pattern changes due to any external stimulus, which could be a change in strain or temperature. In this way, distributed temperature and strain measurements can be obtained by scaling up the spectral and temporal shifts. The accuracy using SWI goes to a very high resolution, enabling robust and practical distributed temperature and strain measurements. The length of the optical fibre can vary from tens to hundreds of meters, which can be resolved over a gage length of millimetre scale. The obtained

temperature and strain measurements can have a resolution of 0.1°C and 1 microstrain respectively.

Talking about the Rayleigh backscatter. Rayleigh scattering analysis is based on optical frequency domain reflectometry (OFDR). As a reference, the Rayleigh scattering pattern occurring along the fibre is initially measured and stored. And when the fibre is subjected to temporal or strain changes, the pattern is saved again. Subsequently, both data sets are divided into small segments that are Fourier transformed into the frequency domain. After comparing the reference and perturbed states, a spectral shift in the correlation peak can be found, which can then be calibrated to the strain and temperature changes [46]. It is generated by randomly distributed fluctuations of the refractive indices inside the core of the fibre. So if there is a shift in the optical path, the local reflected spectrum gets modified, which results in a shift in the backscattered pattern. Thus, Rayleigh backscattering is sensitive to both strain and temporal changes. The measurement range in the case of Rayleigh backscatter is limited to a few hundred meters, but the spatial resolution used to detect the temporal and strain changes is much higher [47]. Figure 26 explains the working principle of Rayleigh Backscattering.

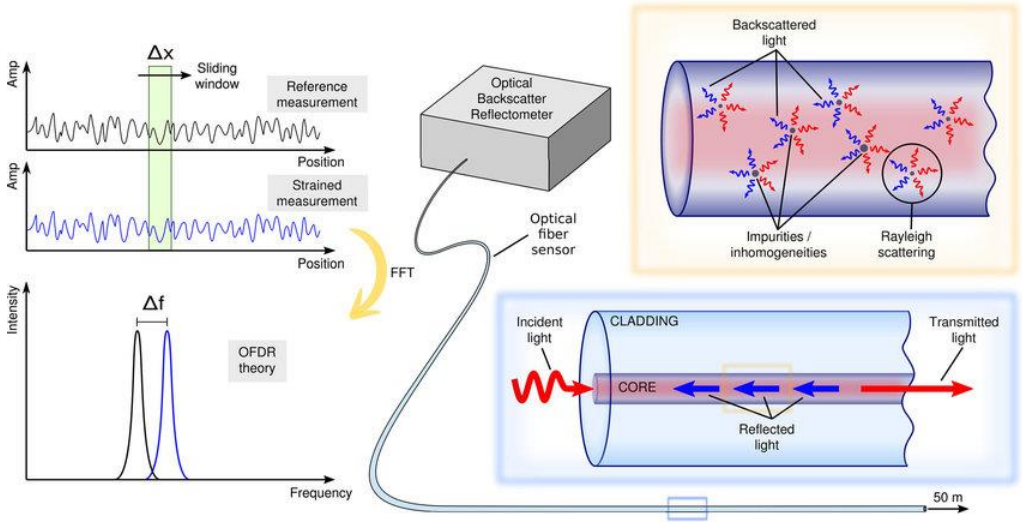

Figure 26 Working principle of Rayleigh Backscatter [46]

Chapter 3: experiments

The experimental phase starts with the preparation of samples to carry out various types of mechanical tests. Optical fibres are the signal-carrying agents that provide us with quite steady and useful data.

The optical fibres have the core as the main element for sensing the changes. That means if the core is placed anywhere in a proper and safe environment, it will indeed provide useful results. It is possible to use the backface (either the top, bottom, or both) of the sample; this is also called backface strain monitoring. Another possibility is to embed the optical fibre inside the joint. When the change in strains is being monitored, a complete shift in the results can be seen while moving from the top via the middle to the bottom of the sample. Therefore, the process can make use of the fibre's presence in the stated places to monitor these changes. To obtain the typical variance of changes between the layers of the matrix, embedding can also be done when the pre-preg layers are arranged into a sample.

The challenges with the fibres start with handling and installing them. Using the optical fibre where the core is made up of glass is mostly preferred since it helps us monitor the variation with utmost effectiveness, but it also adds a risk of the brittleness of the fibre. In the mounting step, glue is used to stick the fibre in the right position, and then paper tissue is used to remove the extra glue that might disorient the surface's smoothness and homogeneity.

3.1 - Instruments and materials.

3.1.1 - Vernier caliper and scale

The basic knowledge of a scale describes it as an instrument used for measuring lengths. The smallest division measurable on a scale goes to a millimetre. But when dealing with carbon and glass fibres the thickness of each layer is of the order of micrometres. Thus, when the samples require stacking of several layers, the usual thickness is never an integral number as a multiple of millimetre scale. Therefore, in that case, a measuring instrument that has better precision and accuracy and can be used to measure thicknesses between millimetres. This is where the vernier scale or vernier caliper comes in.

The Vernier scale has been named after Pierre Vernier. This visual aid utilizes mechanical interpolation to obtain precise measurement readings between two graduation markings on a linear scale. By incorporating vernier acuity, it effectively reduces the possibility of human estimation error, ultimately increasing resolution and reducing measurement uncertainty.

Apart from the linear dimensions, the vernier caliper is also handy for measuring circular dimensions, whether inside or outside, with debatable accuracy. The vernier caliper has been shown below in Figure 27.

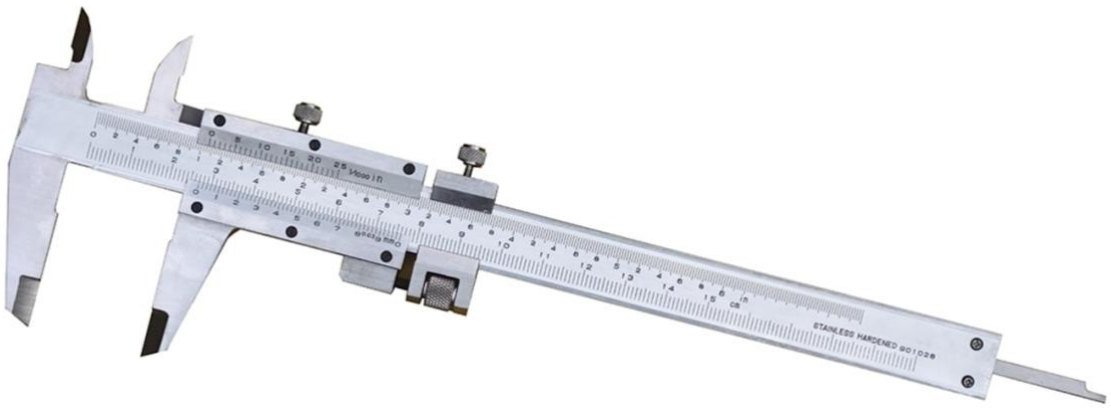

Figure 27 Vernier caliper [48]

3.1.2 - Glass bed

This is the smooth surface used to arrange the layers of the pre-preg in different arrangements as per the requirements of the specimens. The glass bed needs to be thoroughly cleaned for any resin patches from previous experiments. The cleaning process is carried out using paper tissues and ethanol. The use of ethanol ensures no residue owing to its quick evaporation property and thus makes certain that no external sediment remains on the surface to maintain the vacuum properties. It also acts as an antibacterial agent. Figure 28 shows one of the glass beds being used in the laboratory.

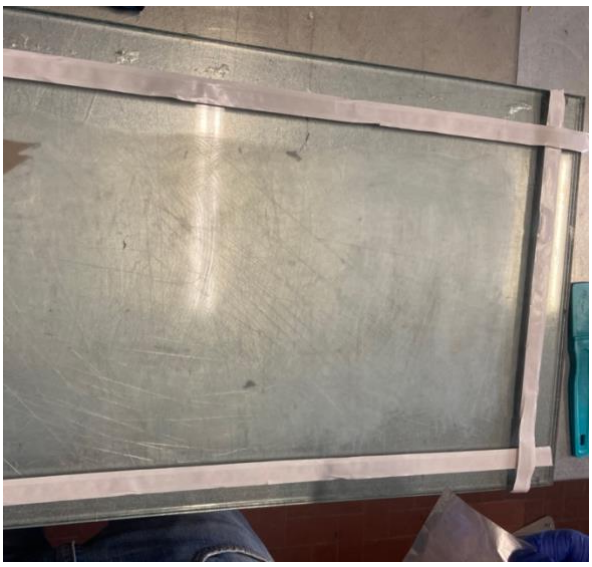

Figure 28 Glass bed

3.1.3 - Wax

The use of wax is one of the most critical aspects of composite manufacturing. It is used to make sure that no damage happens to the glass bed or the sample. Wax creates a layer between the specimen and the bed so that the separation of the two after curing is easy. This is the primary function of wax.

The wax is also used to cover up the optical fibres so that they don't get attached to anything, which would ultimately result in the breakage of the fibre and thus the failure of the specimen since the test cannot be conducted in that case. Below in Figure 29 has been shown the container containing the wax.

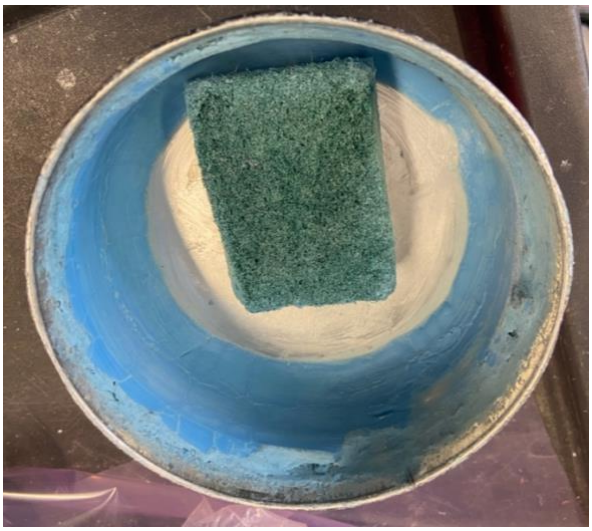

Figure 29 Wax container

3.1.4 - Optical fibres

Two different types of optical fibres from two manufacturers are used in this study. These two differ in their characteristics and dimensions. Both have been discussed here.

- **Polyimide-coated single-mode optical fibre – manufactured by ThorLabs**

Its market name is SM1550P - Single Mode Optical Fibre, 0.12 ± 0.02 NA, 1310 - 1550 nm, Polyimide Coating, Ø125 µm Cladding**.** Since the optical fibre is covered and protected in SM1550P by a layer of Polyimide coating, it can thus be used up to a temperature limit of 350^0C. The limit of the allowable spectrum range of usage in the application of telecommunication is broad, and due to exceptional concentricity between core and cladding, a very high resolution of signals is obtained. Apart from being useful in high-temperature applications, this fibre shows chemical resistance and can be used in a vacuum environment, which makes it an ideal choice for usage in aerospace, medical, and military applications. In Table 2 the general specifications of the optical fibres manufactured by ThorLabs are stated.

Table 2. Optical fibres – Thorlabs [49]

General specifications	
Optical wavelength	1310 - 1550 nm
Numerical Aperture	0.12 ± 0.02
Mode Field Diameter (Nominal)	9.0 µm @ 1310 nm
Core Diameter	9.0 ± 0.5 µm
Core Material	Ge Doped Silica
Cladding Diameter	125 +1/-3 µm
Cladding Material	Pure Silica
Cladding Diameter	145 ± 5 µm
Coating Material	Polyimide
Core-Clad Concentricity	<1 µm
Attenuation	≤0.7 dB/km
Operating Temperature	-190 t0 350 °C

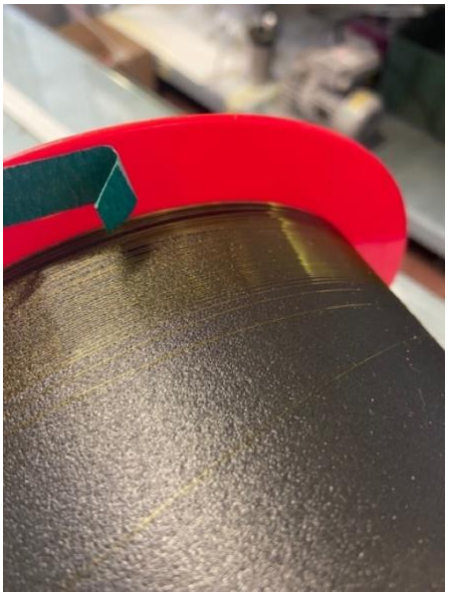

Figure 30. Optical fibres - ThorLabs

.Figure 31. Terminal-ThorLabs

In Figure 30 and .Figure 31 the fibres being used for the experimentation and the terminals have been shown respectively.

- **Single-mode fibre. G.657.A1 200µm – manufactured by Optokon**

In this fibre, the coating is made up of dual layers of UV-cured acrylate. The manufacturer notifies the customer that the length of fibre should be straightened after unrolling from the winding to receive a good response. states the general specifications of the fibres manufactured.

Table 3. Optical Fibre - Optokon [50]

General specifications	
Core	Germanium doped silica
Cladding	Silica, step index and matched clad type
Coating	Dual layers of UV-cured acrylate
Optical characteristics	
Attenuation coefficient Loose tube cables (typical/max) at 1310nm	0.32 / 0.36 dB/km
Point of discontinuity at 1310nm and 1550nm	≤ 0.1 dB
Effective group index of refraction at 1310nm	1.467
Effective group index of refraction at 1550nm	1.468
Effective group index of refraction at 1625nm	1.468
Backscatter coefficient at 1310nm	-79.2 dB
Geometrical Characteristics	
Mode field diameter at 1310nm	8.9 ± 0.4 µm
Core/Cladding concentricity error	≤ 0.5 µm
Cladding diameter	125.0 ± 0.7 µm
Cladding non-circularity	≤ 0.7%
Primary coating diameter(uncoloured fibre)	190 ±10 µm
Primary coating diameter (coloured fibre)	200 ±10 µm
Coating-Cladding concentricity	≤ 12 µm

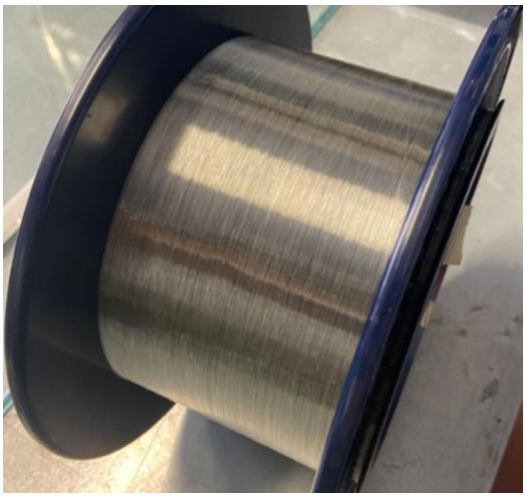

Figure 32 Optical fibre manufactured by Optokon

In Figure 32 the product manufactured by Optokon has been shown. While using these two types of fibres, it was noticed that it is comparatively easier to deal with the Optokon fibre as compared to the one manufactured by Thorlabs. The reason is that the Thorlabs fibre is much more brittle, and utmost care is needed to remove the polyimide coating. However, when the accuracy of results is concerned, the Thorlabs fibre takes the lead and becomes an ideal choice.

3.1.5 - Wazer waterjet cutter

After manufacturing a composite laminate with the desired thickness and characteristics, it has to be cut according to the dimensional requirements of the specimens. For this purpose, a waterjet cutter is used, which is manufactured by Wazer.

The waterjet cutter uses 80 Mesh Alluvial Garnets as an abrasive in combination with water. A separate container is available for storing the abrasive. The cutting bed is made in such a way that the laminate can be fixed to it using screws.

The first step is to make the 2D drawing for the part to be cut. AutoCAD, Solid Works or any other design software can be used to make the drawing with output in .dxf format. This is the proper format for the Wazer online software, wam.wazer.com. This online website provides users with a virtual cutting bed on which the drawing can be imported and positioned. Moreover, from the materials menu, the exact material can be selected or defined. There are several available options to choose from, like metals, plastics, rubbers, ceramics, stone, and

others. Since the process deals with working on composites made of carbon fibre, this material is selected from the "other" option along with the thickness.

The cutting path can be chosen to be centred, outside, or inside the drawing. Choosing the outside path is better, as it helps keep some tolerance for unwanted errors. Finally, the quality of the cut can be chosen. The quality of the cut also affects the time of the operation. After completing all these steps, it is possible to generate the file and save it on the external memory card that goes into the Wazer waterjet cutter.

After programming is finished, the procedure continues with setting up the waterjet cutter. The checks that need to be made are to see whether the cutting bed is clean, the abrasive is filled in the abrasive container, and the water nozzles are open. All these ensure the proper functioning of the machine and a proper cut of the laminate.

Now that all the basic checks have been performed, the laminate should be placed on the machine bed and fixed with screws. Then the prepared program cut should be chosen. Before starting the cut, first, the position of the nozzle should be manually defined, i.e., where to start the cut on the laminate. The "dry run" option in the machine menu enables users to see exactly the cut path and ensures that the real cutting will be error-free. Finally, by closing the lid of the waterjet cutter, the cutting operation can be started. The machine will show the time left for the operation to be finished. After the cutting process is finished, the specimens can be taken for any final touch-ups, and sandpaper can be used to make the samples dimensionally correct if an error is greater than the allowed tolerances.

Figure 33. Wazer Waterjet cutter

Figure 34. Cutting bed

Figure 33 and Figure 34 show the waterjet cutter available in the lab and the bed on which samples are fixed to be cut respectively.

3.1.6 - Splicing, fusion and termination

Splicing is the process of joining two fibre optic strings together. This process can be used to repair a damaged fibre, elongate a fibre, attach a fibre to a pigtail, or make a terminal.

There are two open ends in fibre, one of which will go into the acquisition system and one of which will be the end also called the terminal. The end that goes into the acquisition system is spliced with a pigtail. Pigtails are required to connect the optical fibres to the patch panel or the acquisition system. However, before splicing, the fibre needs to be cleaved, which involves removing the coating from the fibre and then using a cleaver to cut the fibre so that there is a proper surface for fusion. The cut has to be straight in angular precision; otherwise, the information loss will be far greater than the allowable limit. Figure 35 and Figure 36 show a working model of the cleaver in open and closed configurations used in the lab.

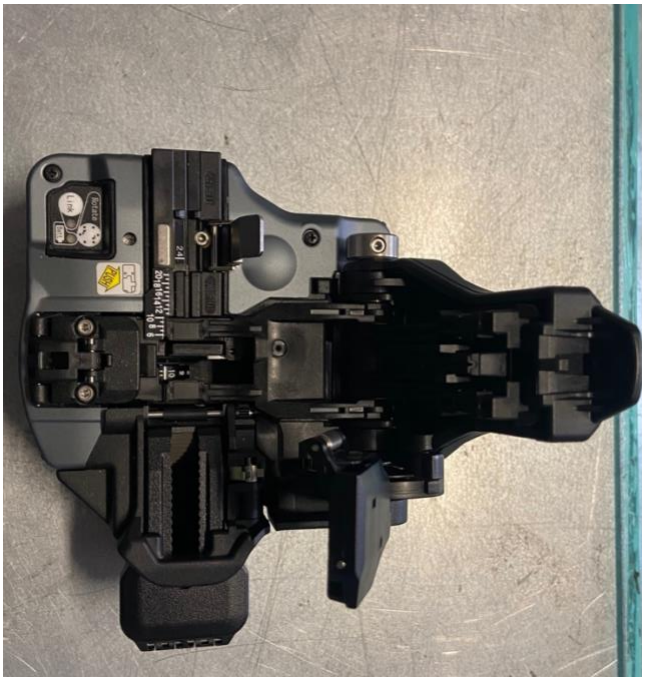

Figure 35. Cleaver – Open

Figure 36. Cleaver - Closed

Figure 37. Splicer with User Interface

Figure 38. Splicer - Top view

Fujikura 90S+ is the splicer being used as shown in Figure 37 and Figure 38. Before starting the process of splicing the fibres, it has to be made sure that the flatness of the cut surface is appropriate and that the fibres are clean of any dust. Otherwise, the splicer will not fuse the fibres and the machine will show an error without finishing the operation. The cleaning of the fibres is performed using cotton tabs and isopropyl alcohol as the cleaning agent.

The two fibres that are to be spliced are placed close to each other. A motor is internally working in the splicer, which brings the two fibres close to being fused. The fusion process also depends on the alignment of the fibres with respect to each other, and after all these constraints are overcome, the splicing process happens. The process can be viewed through the user interface, which operates using the in-built camera in the device.

Figure 39, Figure 40, Figure 41 and Figure 42 describes the fusing in case the alignment is proper and in case there had been any issues while cleaving the fibres.

Figure 39

Figure 40

Figure 41

Figure 42

Also regarding the fibre junction area, where the two fibres are attached, it can be either covered with a protective layer of plastic or left naked. Usually, if the test is going to be conducted within a short period after the preparation of the specimen, it is suggested to leave it naked

because it does not affect the quality of the received spectrum as such. Otherwise, it is better to keep the junction covered.

Figure 43 shows a protected junction with the plastic layer covering the optical fibre junction. The application of this protective layer requires the heating of a hollow cylindrical plastic covering when placed at the location of the junction. The splicer is used for this function too.

Figure 43 Plastic covering the fibre joint for protection

3.1.7 - DIC system

The digital image correlation (DIC) system is a non-contact testing technique used to measure changes in displacement and, consequently, strain characteristics on any surface. In this study, the DIC system is used along with LUNA Odisi-B as a data acquisition system. This will help us realize the correctness of the measurement of the results since the process needs to have equivalent results from both.

The setting up of the DIC system is a time-consuming and cumbersome process. It involves a lot of parts that have to be put together for the proper functioning of the system. Some of the main components of the DIC system are the acquisition system or the data gathering system,

which has to be connected through proper channels to the highly sensitive cameras. Moreover, it has to be synchronized with the Instron machine so that both acquisition systems read the same data. In addition, the lenses should be chosen carefully so that they can provide us with images that are properly focused and have a very fine quality. This can be done by using Mavic software, which is installed on the DIC computer. The cameras used in the DIC system can vary in number depending on the subject and the user's will, as it is possible to perform 2D or 3D image acquisition and analysis.

Regarding the samples, they should be prepared at the location of interest by using painting spray cans and creating random patterns in white and black. The process is very delicate, as this pattern will be used to track the changes on the surface of the specimen using postprocessing software like VIC_3D.

Before starting the experimentation on the DIC, the cameras must be calibrated. This is done to ensure that the error in gathering data collected through pictures is as low as possible. Figure 44 and Figure 45 show the calibration of the DIC being done using some standard patterns. These standard patterns are imitations of the real samples.

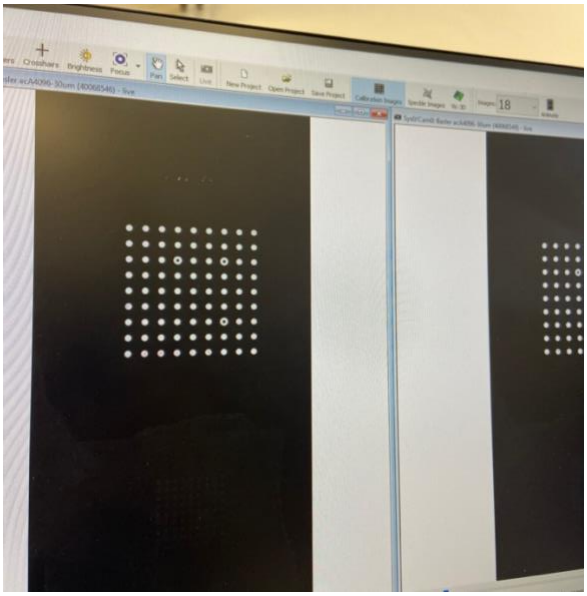

Figure 44. DIC Calibration I

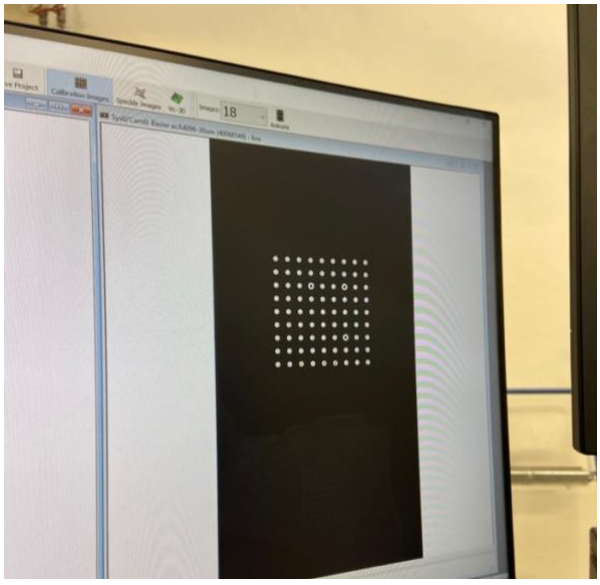

Figure 45. DIC Calibration II

Furthermore, it has to be made sure that the component of noise in the pictures that are captured is as low as possible. In other words, it can be called keeping the image focused in the best

possible manner, and the pattern formed by painting the sample is evenly distributed. The noise is denoted by a colour distribution that runs from purple to red, where purple is the best-case scenario, as shown in Figure 46 and Figure 47. In case the focus is not good, the colour will be red.

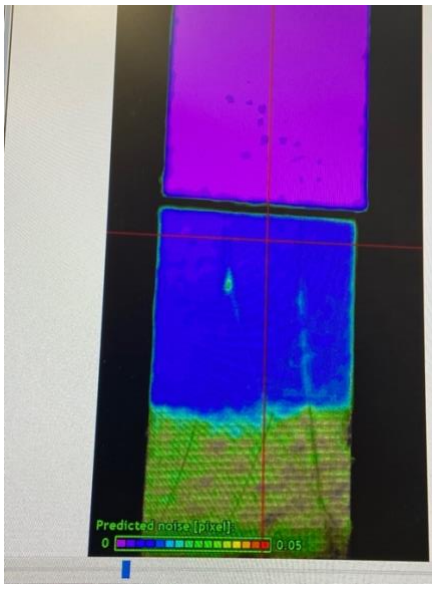

Figure 46. noise reduction I

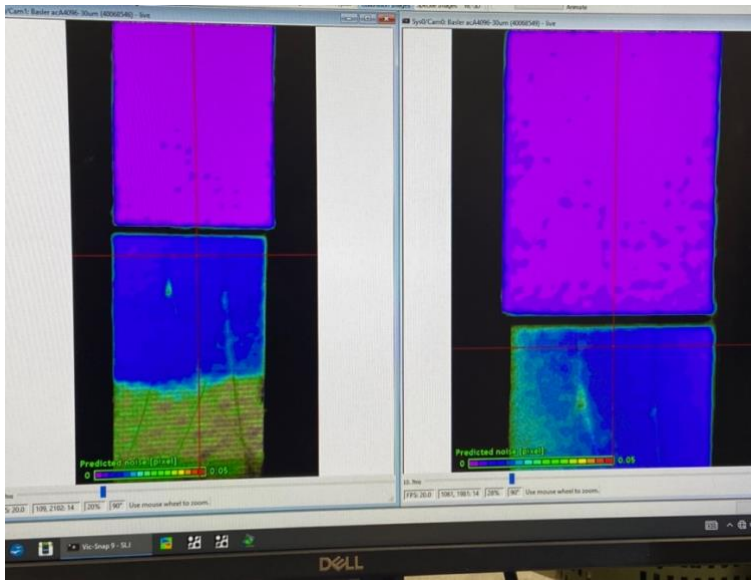

Figure 47. Noise reduction II

3.1.8 - Instron 8801

Instron is one of the most commonly used tensile testing machines inside laboratories. It's one of the most fundamental types of mechanical testing instruments in use and is used to find out the material properties of the component and the specimens. Force and displacement are the two most common quantities that Instron provides users with. The former is measured using the load cell installed on the upper fixed jaw of the machine, while the latter is measured by monitoring the movement of the moving jaw. This machine works using a hydraulic pump and a series of computer-controlled valves that maintain the pressure inside the lines. Due to the heavy weight of the machine, the base is installed on the floor with a damper installation to minimize the disturbance due to the vibrations. It also makes sure that other instruments, which are usually sensitive to vibrations, function properly. Figure 48 shows the Instron machine that is being used in the lab.

Figure 48 Instron 8801

3.1.9 - Luna Odisi 6100 series

The Odisi 6100 series is a multichannel acquisition system that can be used to monitor changes in strain and temperature during mechanical tests. It's a highly sensitive setup using optical fibres for acquisition. It's a very high-definition measurement setup considering the least [0.65mm] of gage length which can be used in data collection, ensuring thus a very high spatial accuracy compared to the conventional strain gauges. The manufacturer of the Odisi series is LUNA, and it is used in different industrial setups ranging from defence, aerospace, optical equipment manufacturers, fibre optics, etc.

The version that is used in the lab is LUNA Odisi 6102. The whole package includes an optical distributed sensor interrogator, a dedicated instrument controller, some standoff cables, remote modules, a connector cleaner, and some charging cables.

To set up the whole system, an order needs to be followed, which will form a closed circuit. In this circuit, the optical fibre, connected to a terminal at one end and to the pigtail on the other, acts as the signal-transferring agent, which records the strain change in the specimen. The pigtail is connected to the remote module [Figure 50] which via the standoff cable [Figure 49]

goes to the acquisition board [Figure 52]. The acquisition board connected to the controller [Figure 51] (laptop) completes the circuit.

One of the most important aspects that has to be kept in mind is the cleaning of the connections. For that reason, a dedicated connector cleaner [Figure 53] is sent along with the whole setup by the manufacturer. This is used to clean the pigtail end and the ends of the standoff cable. It has been observed that the final reading if taken without cleaning the connections, is much less clear and certain.

Figure 49. Standoff Cable

Figure 50. Remote Module

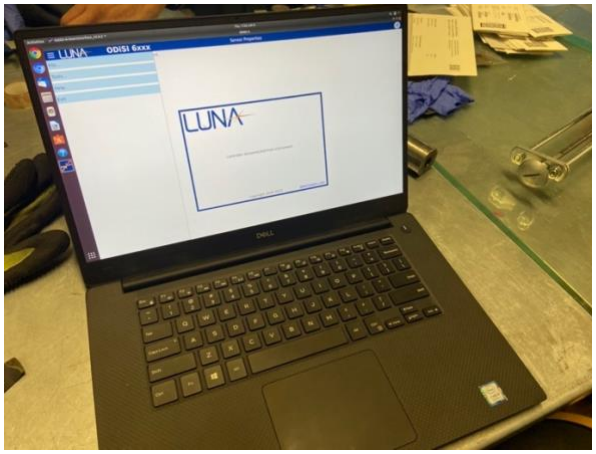

Figure 51. Controller

Figure 52. Acquisition Board

Figure 53. Connector cleaner

The first step after the physical setup is to check whether the fibre connection is working properly or not. This is important since the optical fibre is very sensitive and the connections made with the pigtail and the terminal need to be ensured. This step is an important pre-requisite and helps in the detection of the signal transferred, the loss of termination, and fibre breakage. As can be seen in Figure 54, the signal towards the terminal of the fibre is low, and although the termination has been done and the complete circuit has been formed, the results won't be as expected. This is an example of the use of Optokon Fibres. In this case, it is better to make a new connection and then try to check for quality again.

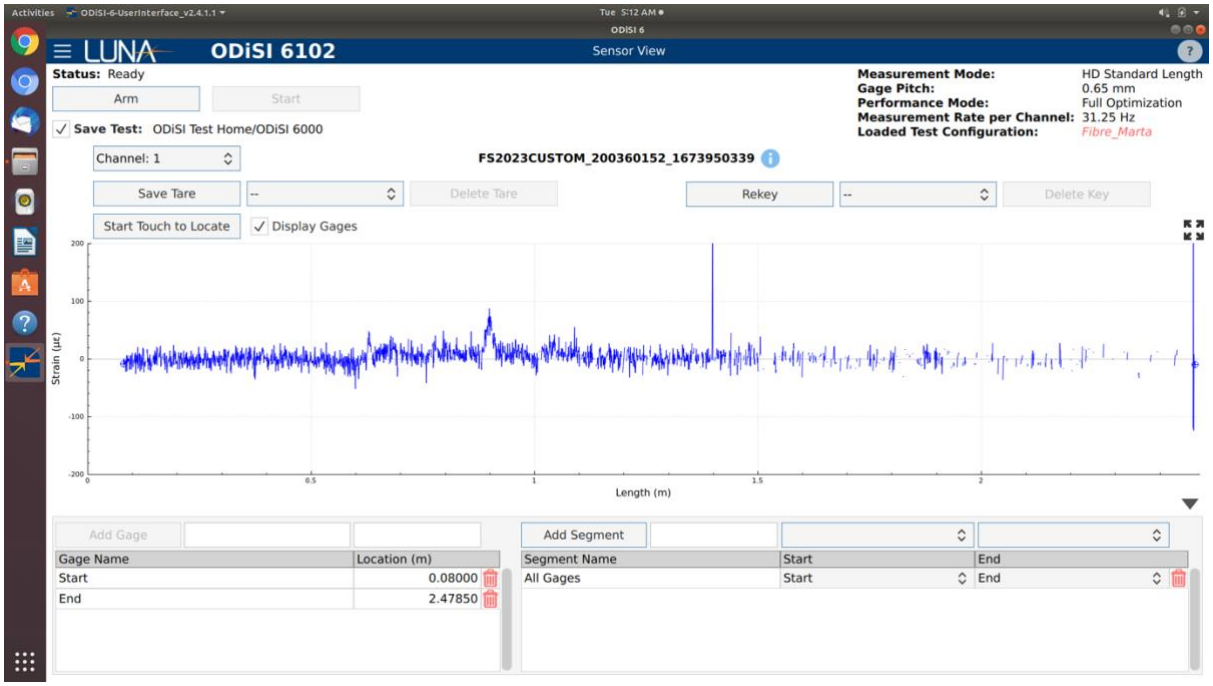

Figure 54 Sensor view showing the passage of the signal through one of the Optokon fibres

One of the most important parameters in terms of measurement is the gauge length. Owing to the high sensitivity and accuracy of the system under discussion, the lowest possible gauge length is 0.65 mm. In simple words, gauge length can be defined as the minimum distance between two points where data can be acquired by the system. The gauge length can be further increased in integral multiples of the minimum gauge length allowed by the system, i.e., 1x0.65, 2x0.65, 3x0.65, and so on, according to the span of the specimen and the sampling requirements. The frequency of acquisition is automatically selected by the controller as either 20 Hz, 32.5 Hz, or 62.5 Hz, depending on the length of the optical fibre. The frequency of acquisition of Luna Odisi-B should be accurately matched with that of an Instron or DIC acquisitor. This makes the final data analysis easier.

3.2 Sample manufacturing and material

The process demands manufacturing samples for shear tests on single-lap joints. The adherends have been made of pre-pregnated carbon fibre-reinforced polymer. For variations in thickness between different samples, the number of CFRP layers used was changed. Adherends were bonded together using adhesive. The CFRP used in this experiment is an epoxy prepreg woven and is marketed as XPREG XC130. This prepreg is uncured 2x2 twill, which requires an oven or an autoclave for the curing process. The product description of this prepreg requires a storage environment of -18 ^{o}C and it always needs to be kept in sealed packaging. The adhesive employed for the experimentation is a polyurethane named ADEKIT A236/H6236. A total of 8 samples have been prepared in such a way that 4 pairs of samples were obtained. The variation of samples is done based on the layers of prepregs in the adherend and the overlap length. Table 4 shows the detail of the different samples which we have used for backface strain monitoring.

Table 4. Samples used in backface strain monitoring

Sample name		Adhesive thickness [T_a(mm)]	Overlap length [L_a(mm)]
Reference	L2W2T2	1.3	20
Sample 9	L1W2T3	1.37	10
Sample 10	L1W2T3	1.37	10
Sample 11	L2W2T3	1.36	20
Sample 12	L1W2T2	1.67	10
Sample 13	L2W2T3	1.4	20
Sample 14	L2W2T2	1.13	20
Sample 15	L1W2T2	1.51	10

In Table 4 the names have a particular meaning and act as standard names for identifying the specimen. "L" denotes the overlap length, which has been kept at either 10 mm or 20 mm. Similarly, "W" denotes the width of the specimens. For the experimentation, the width has been kept at a constant value of 20 mm. "T" denotes the thickness of the adherend, which changes according to the number of layers being used in the adherend. The number of layers of the prepreg in samples with thickness T2 is 4, while in those with thickness T3, it is 8. Each layer has a consolidated thickness of 0.25 mm.

The characteristics of adhesive polyurethane (ADEKIT A236/H6236) can be changed. Its properties vary according to the ratio of binder and hardener being used. Usually, the ratio required for assemblies or any other usage is already fixed by the manufacturer, and the details are provided in the data sheet. The data sheet is a very important document, as it has all the details not only about the mixing proportion but also the cycles of curing required. ADEKIT A236/H6236 has a mix ratio (by weight) of 92 parts of POLYOL to 100 parts of ISOCYANATE and a mix ratio (by volume) of 100 parts of POLYOL to 100 parts of ISOCYANATE. This should always be kept in consideration while setting up the resin gun so that the final results come as per those defined by the supplier.

The adherends are cut according to the specified dimensions, as shown in **Error! Reference source not found.**, from a larger laminate sheet which was prepared and cured inside the oven. After cutting using the Wazer waterjet cutter and proper cleaning, a final thickness measurement should be done. As the thickness is measured, the required adhesive thickness is also fixed. And thus, according to the sum of the adherend and adhesive thickness, a tab is chosen that acts as support below the adherend on the top of the lap joint. This is a very necessary step to ensure a constant thickness of the adhesive layer for the joint.

The nozzle of the gun, used to pour the adhesive on the joint location, should be kept as close to the surface as possible. This ensures that no air bubble is trapped between the adhesive which otherwise would result in a change in the characteristic properties of the joint and loss of strength too. After putting some amount of adhesive and spreading it as evenly as possible the top adherend is put onto the joint location. A metallic tab with a width two to three times more than that of the lap joint is put over the joint as shown in Figure 56. One end of this metallic tab is put just at the end of the lap joint and then it goes back eventually making the even thickness of the joint possible.

The samples are left to cure at room temperature for 24 hours. After this curing is finished, the samples are put inside the oven for 16 hours and kept for curing at an elevated temperature of 70^{o}C. These cycles of curing have been mentioned in the datasheet for the adhesive provided by the supplier.

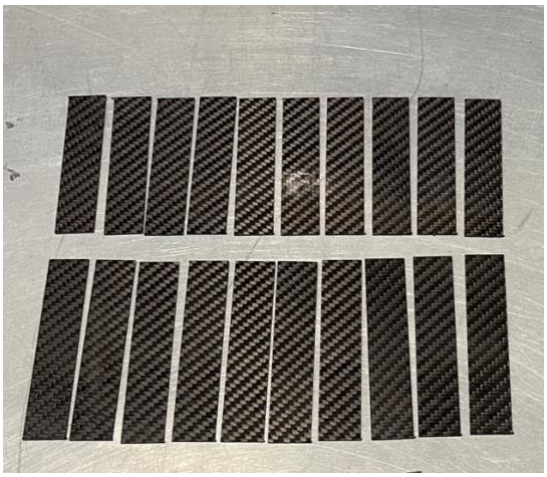

Figure 55. Cut out CFRP samples

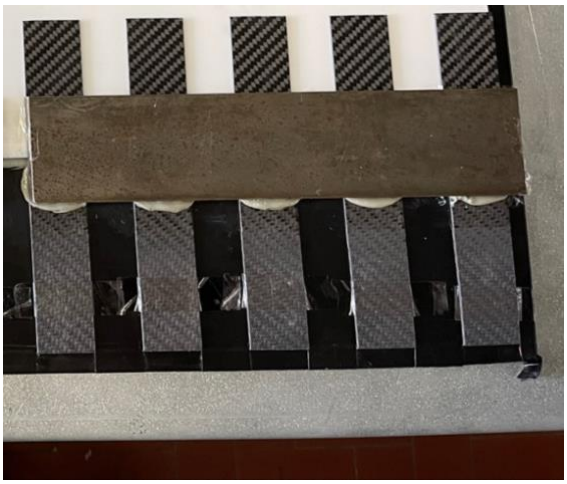

Figure 56. Preparation of SLJ samples for back face strain monitoring

Before beginning the tests, optical fibres have to be attached to the surface of the lap joints. For this process, both faces of the specimens have been used, as shown in Figure 57. The optical fibre manufactured by ThorLabs has been used for this process, owing to its higher accuracy and precision. A single optical fibre has been used in such a way that by winding it above and below the joint, a total of four places of attachment have been obtained. This has been done to ensure the repeatability and comparability of the results. For attaching the fibres Attack Glue can be used. Before attaching, the fibre must be maintained in a tensile position in such a way that in the area of interest, the fibre is straight and without any bends. Figure 57 shows a schematic describing how the optical fibre goes along the surfaces of the single lap joint. One end of this fibre is made into a terminal, while the other end is attached to the pigtail, forming connections with the other components of Luna Odisi-B to be built into a circuit.

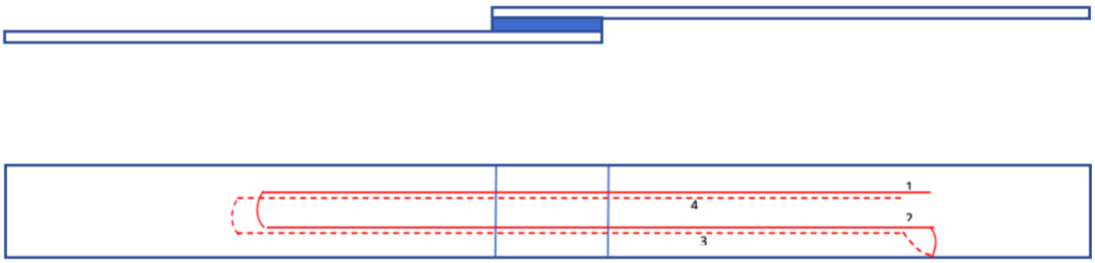

Figure 57 Schematic of the Backface strain monitoring SLJ specimen

As already mentioned in the section dedicated to Luna Odisi-B, the fibre attachment is followed by a necessary check to make the working condition of the fibre certain. Figure 58 shows the

frequency domain reflectometry plot for one of the samples. In this figure, two red crests can be seen. These crests denote the beginning and end of the connection, and since these are visible, it means that the connections between the optical fibre-pigtail and optical fibre-terminal are detected properly by the acquisition board. The plot in between these two red crests is where the testing, experimentation, and results will be generated.

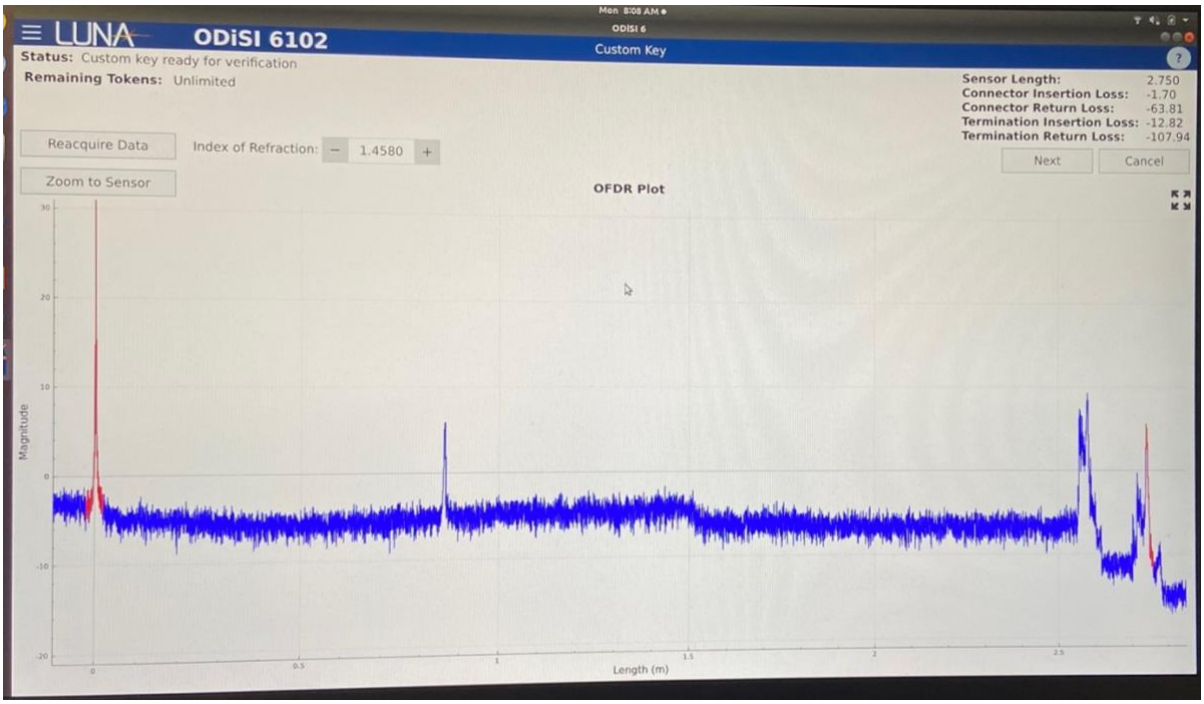

Figure 58. OFDR plot for one of the samples

3.3 Test setup

The test setup primarily involves three main machines: 1) Instron 8801. 2) DIC system. 3) Luna.

While both DIC and LUNA are the data acquisition systems, Instron is the one that gives us the load and displacement curves. The samples before the main testing are to be painted so that the DIC acquisition is possible. The paint is done using white and black sprays, making a base layer of white paint over which black paint is sprayed so that a dotted pattern is seen at the area

of interest. Figure 59 shows one single lap joint specimen which has been painted for DIC acquisition.

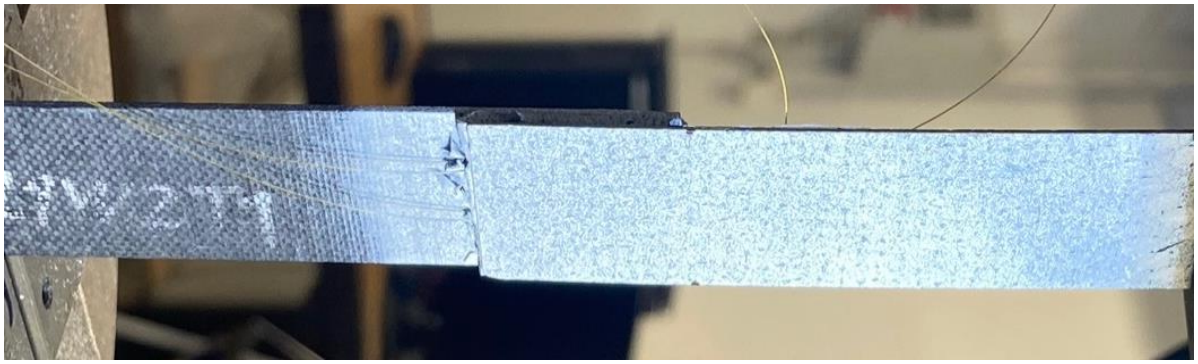

Figure 59. Spray patterned specimen

One end of the fibre is used as a terminal, while the other end is used for measuring the strains using the test setup and the acquisition system. Figure 60 shows the sample fixed inside the upper fixed jaw of Instron. It's kept free from the lower jaw until the position of the lower jaw becomes equivalent to the end tab where it needs to hold the specimen. Figure 61 and Figure 62 show the cameras of DIC focused on the area of overlap of the joint where the strains are to be measured. Once the position of the DIC has been fixed, any accidental movement will make the whole process of calibration go in vain. Thus, utmost care is taken to prevent this from happening.

Figure 63 shows the sample where both the jaws have been fixed and a closer look at the sample.

Figure 60. Sample Loaded on Instron

Figure 61. DIC I

Figure 62. DIC II

Figure 63. Closer view of Instron with sample

On the Bluehill software of Instron, the option "sample protect" is chosen, limiting the load up to 200 N before fixing the lower jaw. This ensures that the sample is not damaged, preloaded, or displaced before starting the test. After this is done, the load is manually reduced to keep it as close to zero as possible.

The pigtail is connected to the LUNA Odisi-B. The specimen is selected inside the controller of LUNA after checking the signal properties, which should show a continuous result as shown in Figure 64. Then the specimen is armed, and the file name is given. After arming the specimen, the final step that remains is to start the test, but once again, the acquisition frequency between the Instron and Luna should be checked and made equal.

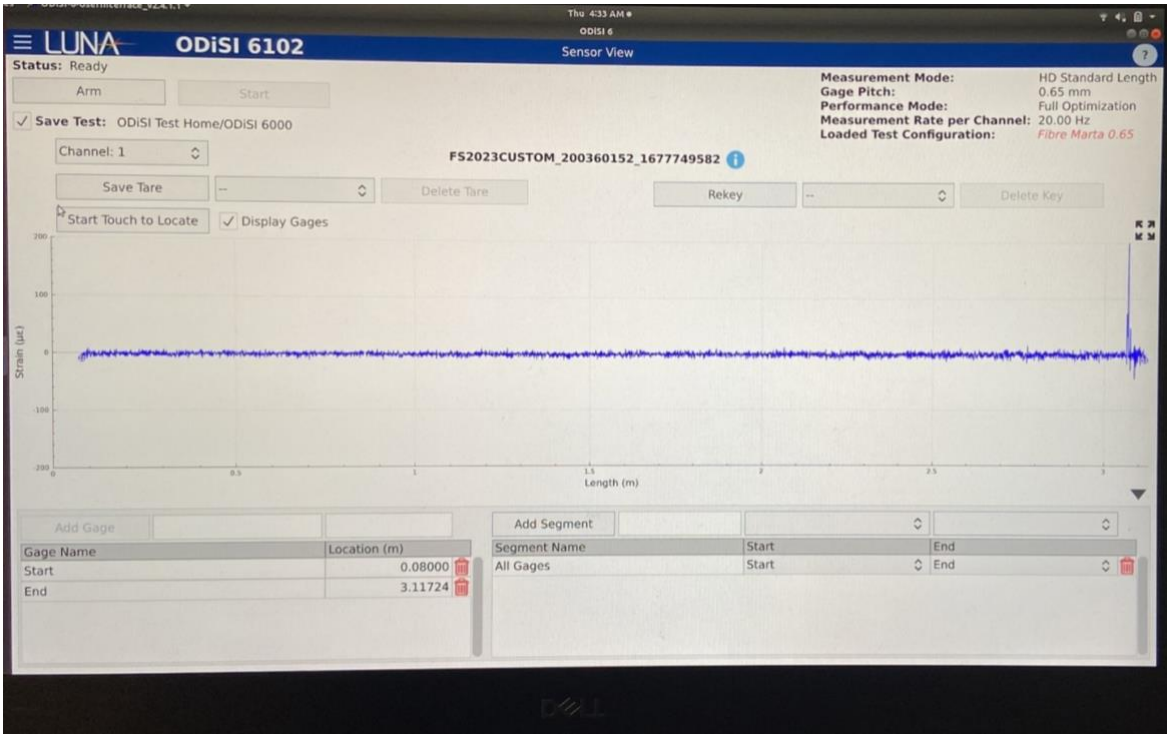

Figure 64 Sensor view showing the passage of signal from the ThorLabs Optical fibre used for our samples

After everything is ready, the acquisition is started on DIC and LUNA at the same time as the load cell starts working on the Instron. Data is acquired, saved, and later analysed using Excel and MATLAB.

Chapter 4: Results and Discussions

The discussion about the results obtained from the samples where back face strain monitoring is done on both faces of the lap joint is shown here. In the specimens, one face is kept towards the DIC cameras while data is simultaneously being acquired by LUNA too, so that the results from both are available to compare. Out of the two types of fibres, this process involves using polyimide-coated optical fibre manufactured by ThorLabs, owing to its enhanced clarity and accuracy. In Figure 65, Figure 66, Figure 67, Figure 68, Figure 69, Figure 70, Figure 71 and Figure 72, the damaged surfaces can be observed.

It can be seen from these surfaces that the type of damage occurring varies characteristically. In some cases, a clean mid-section crack with almost adhesive peeling can be seen, while cohesive damage is evident in others with an inaccurate crack location.

There could be many reasons for the behaviour observed, like the creation of a moment due to the difference between the end tab thickness and the step lap thickness. Additionally, since the process of making the joints is manual, there is an obvious chance of human error, which can also come into play while cleaning the joints off the extra adhesive. Sometimes the roughness of the adherend is not equivalent all over the area of overlap, resulting in differences in behaviour.

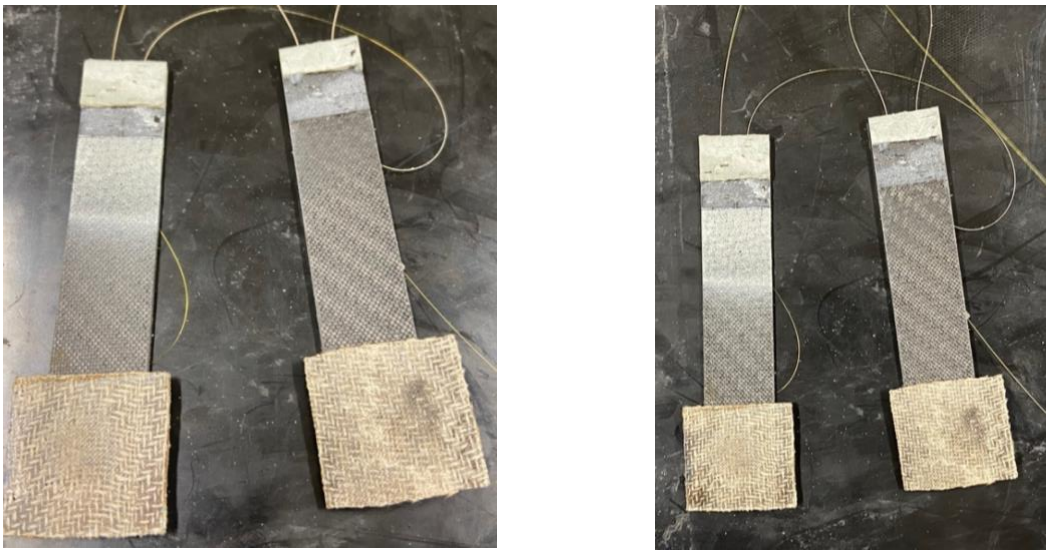

Figure 65. Reference sample with 20mm overlap

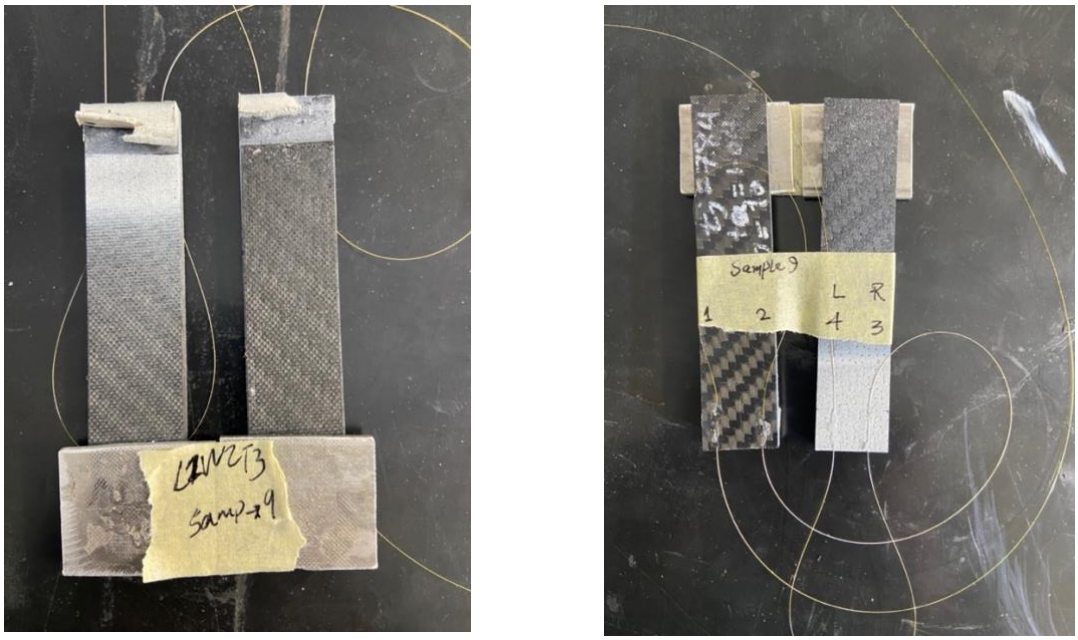

Figure 66. sample 9 with a 10 mm overlap

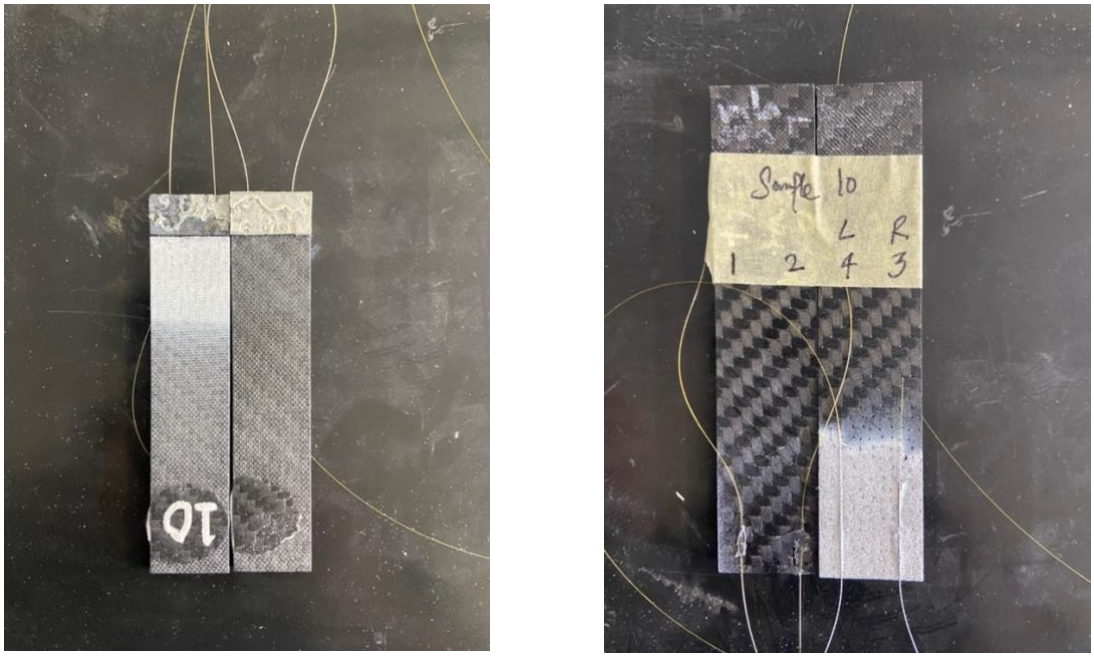

Figure 67. Sample 10 with a 10mm overlap

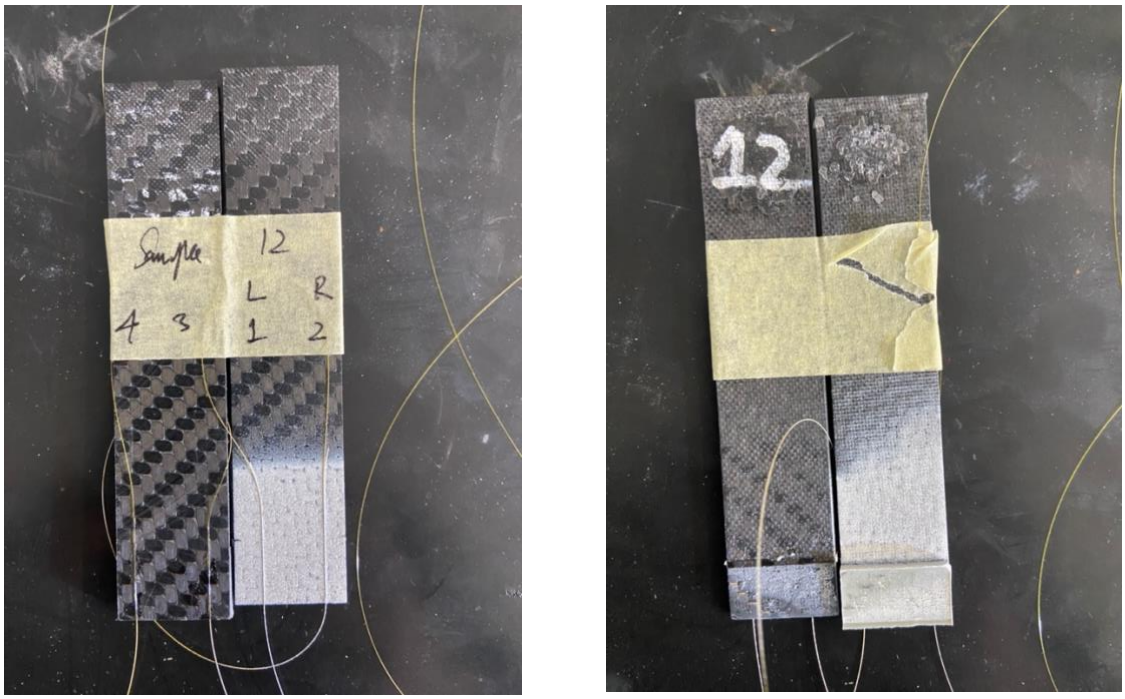

Figure 68. sample 12 with a 10mm overlap

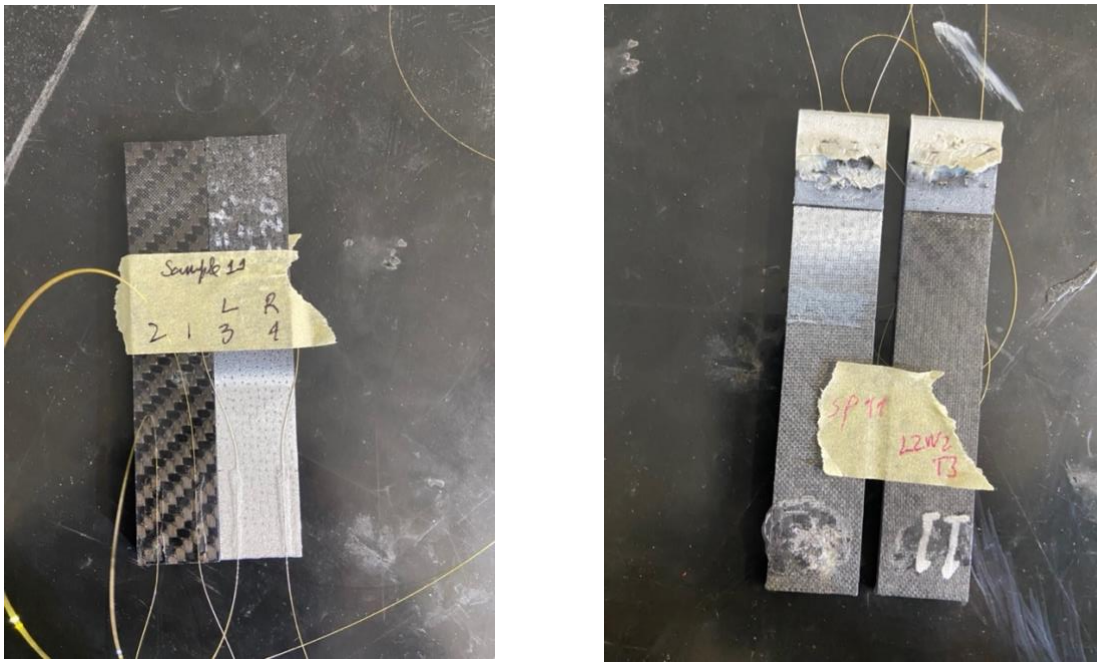

Figure 69. Sample 11 with 20mm overlap

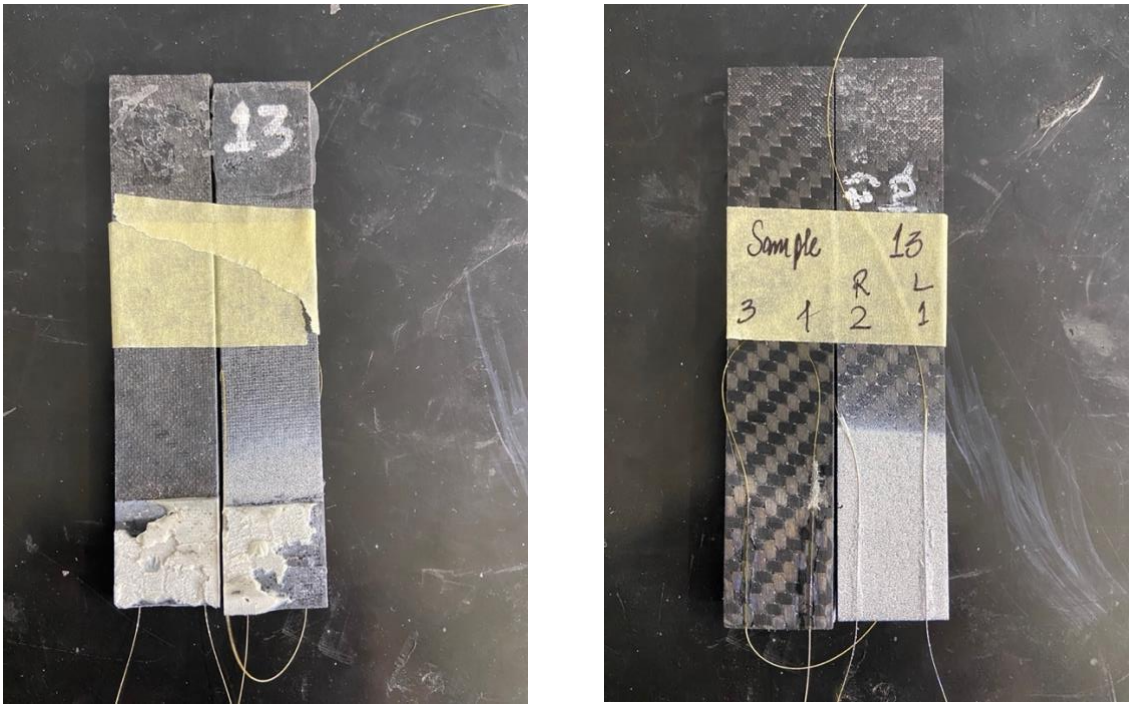

Figure 70. Sample 13 with 20mm overlap

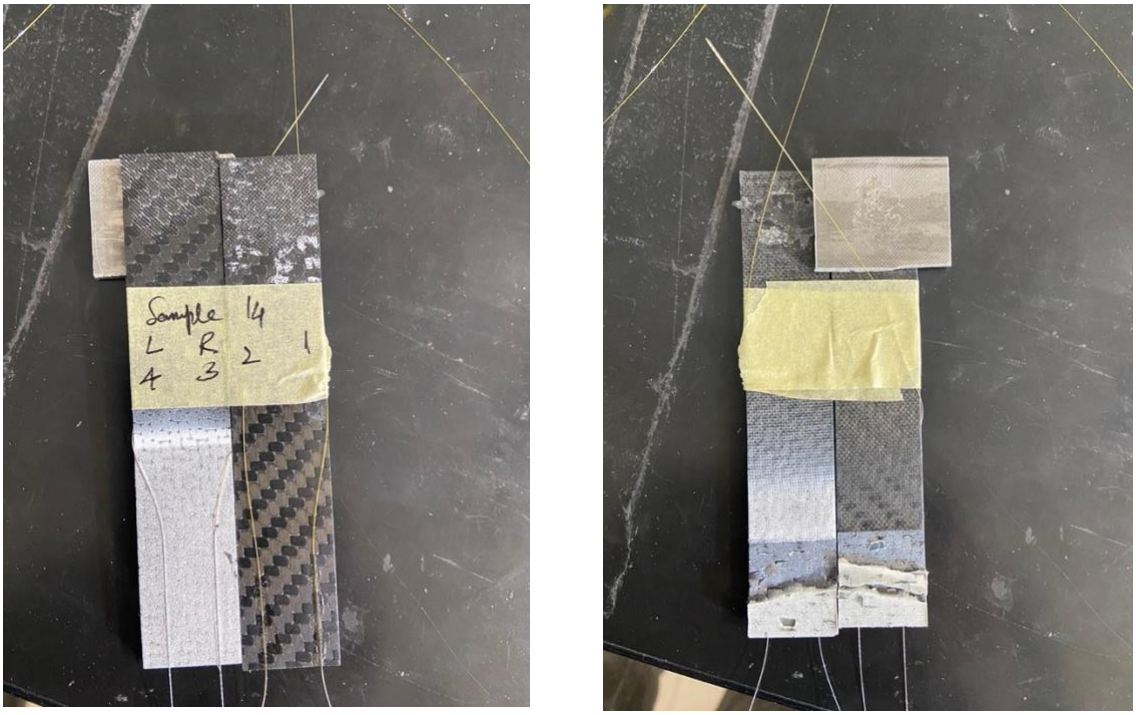

Figure 71. Sample 14 with 20mm overlap

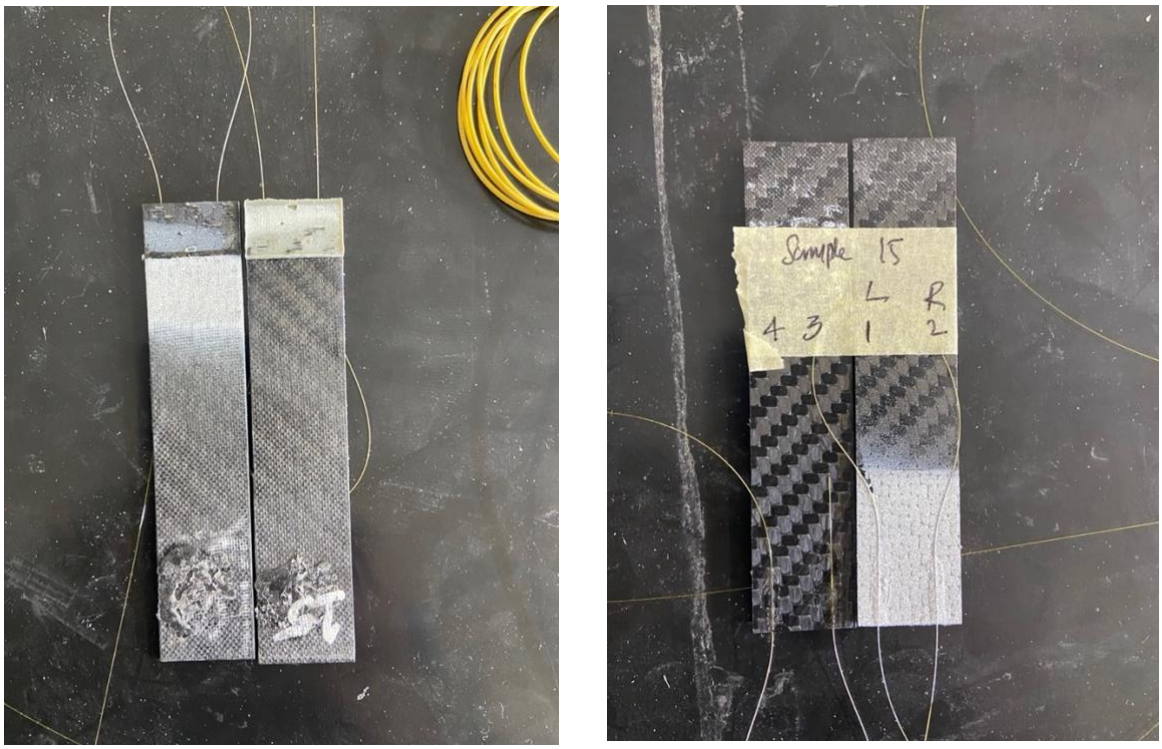

Figure 72. Sample 15 with a 10mm overlap

All the figures above show the damage propagation during the shear loading of the lap joint. Apart from the visual inspection, the results can also be taken from the data acquired from the acquisition systems. For the four pairs of samples, the results can be summarized individually as well as together.

Results that are not easier to define using visual inspection can be guaranteed through data. This includes the maximum amount of loading up to which the joint stays as it is, the time in which the value of strain changes from zero to the point of failure or breakage, and the location of maximum strain. All these characteristics will vary with the strength or type of joint. Additionally, results will also show changes if the curing process or the manufacturing process has caused any differences between the specimens.

Now coming to the strain, loading magnitude, loading time, and position of maximum strain along the joints. In Figure 73, Figure 74, Figure 75, Figure 76, Figure 77, Figure 78, Figure 79 and Figure 80 representation has been shown for the characteristic change between strain and time in a given specimen while it is being loaded and strain at a particular load over the length of the overlap. It can be observed that, apart from negative peaks in the strain vs. length curve,

small positive peaks can be seen too. This is a result of the difference between the end tab thickness and the step thickness of the lap joint, as discussed earlier. Additionally, the variation of strain characteristics is different in different specimens; the reason leading to these results is because of the surface properties such as straightness and roughness of the adherends, which, as a reason for dependence on manual operations, could indeed vary from one specimen to another. The span of the length for which strain change can be seen is sometimes greater than the actual length of the joint; this could be because of the attaching process using glue, which could have attached a little more of the fibre to the surface than the actual length of the joint. Also, when the load is exerted on the specimen, the strain, because of shear, starts a little bit before the actual start of the joint.

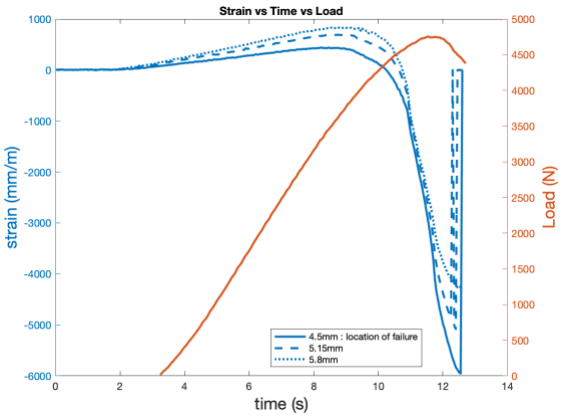

Figure 73. Reference sample[strain vs load]

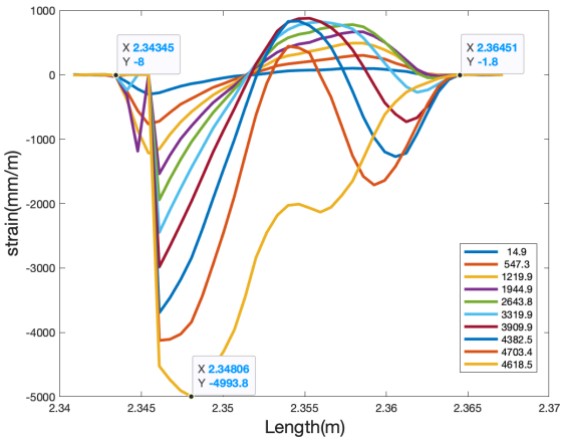

Figure 74. Reference sample[strain vs length]

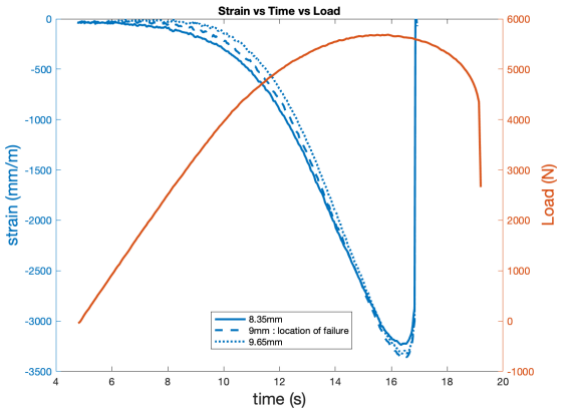

Figure 75. Sample 11[strain vs load]

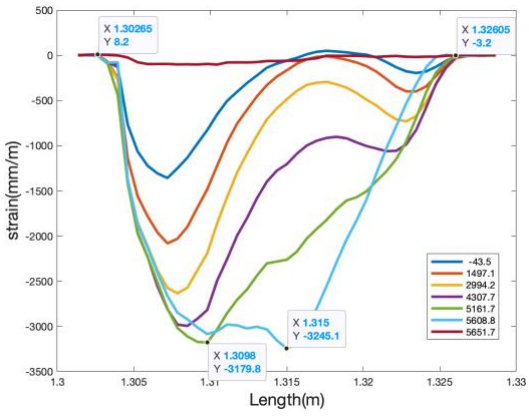

Figure 76. Sample 11[strain vs length]

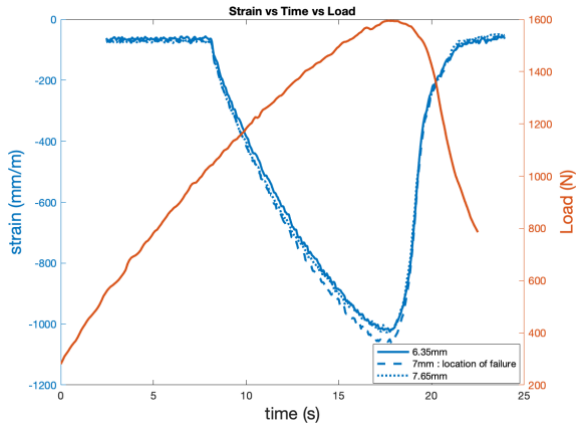

Figure 77. Sample 10[strain vs load]

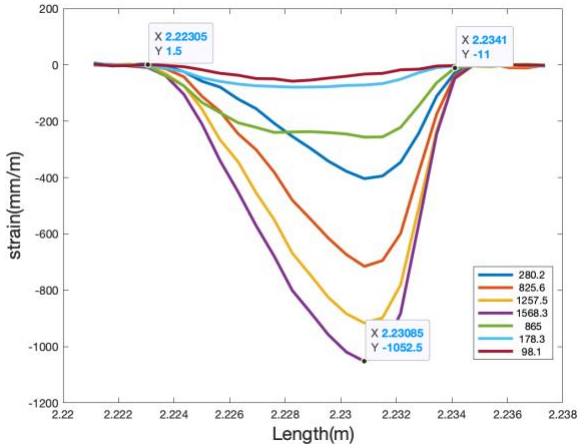

Figure 78. Sample 10[strain vs load]

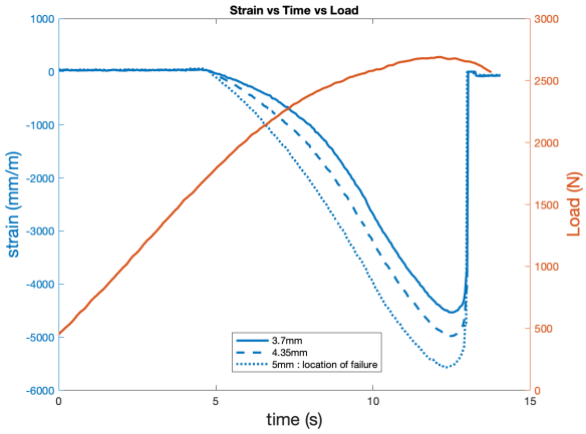

Figure 79. Sample 15[strain vs load]

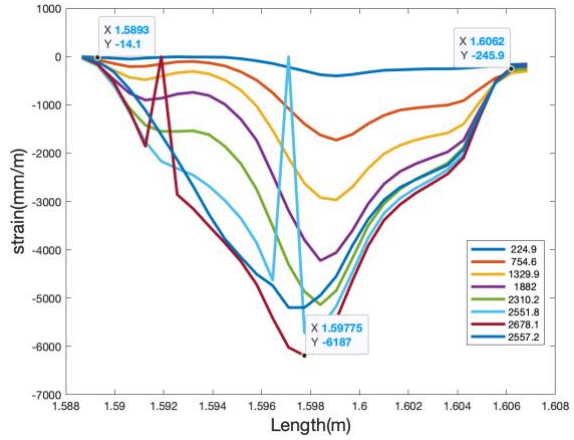

Figure 80. Sample 15[strain vs length]]

The loading curve (in red) is representative of Instron, and the strain leading because of that has been shown only near the peak point where peak strain is observed and a couple of gauge points along the vicinity of that location. The location of the peak strain has been found from the strain vs. length characteristic diagram. In this way, an almost precise location of the maximum strain point can be found, and it is possible here only because of the use of optical fibres. Had the experimentation taken into account the use of strain gauges, the gauge length could never have reached the minimum value available in the case of optical fibres.

When analysing the strain vs. length curves in the composite specimens, it was observed that a large number of curves were not good enough to be considered, which led to the critical thought of performing experiments to check the effect of the surface properties on the strain

results obtained from optical fibres. Additionally, in the curves of strain vs. length for composites, the point of maximum strain is not properly defined.

To address these issues, similar tests were performed on steel samples with much smoother surface properties as compared to the composite specimens. Figure 81 and Figure 82 show the characteristics of strain as seen on testing the samples made of steel. The number of curves is so great because, at every point in the length of the SLJ made of steel, we get better results owing to the surface texture. Also, the point of maximum is properly evident here, unlike in the cases of composite samples.

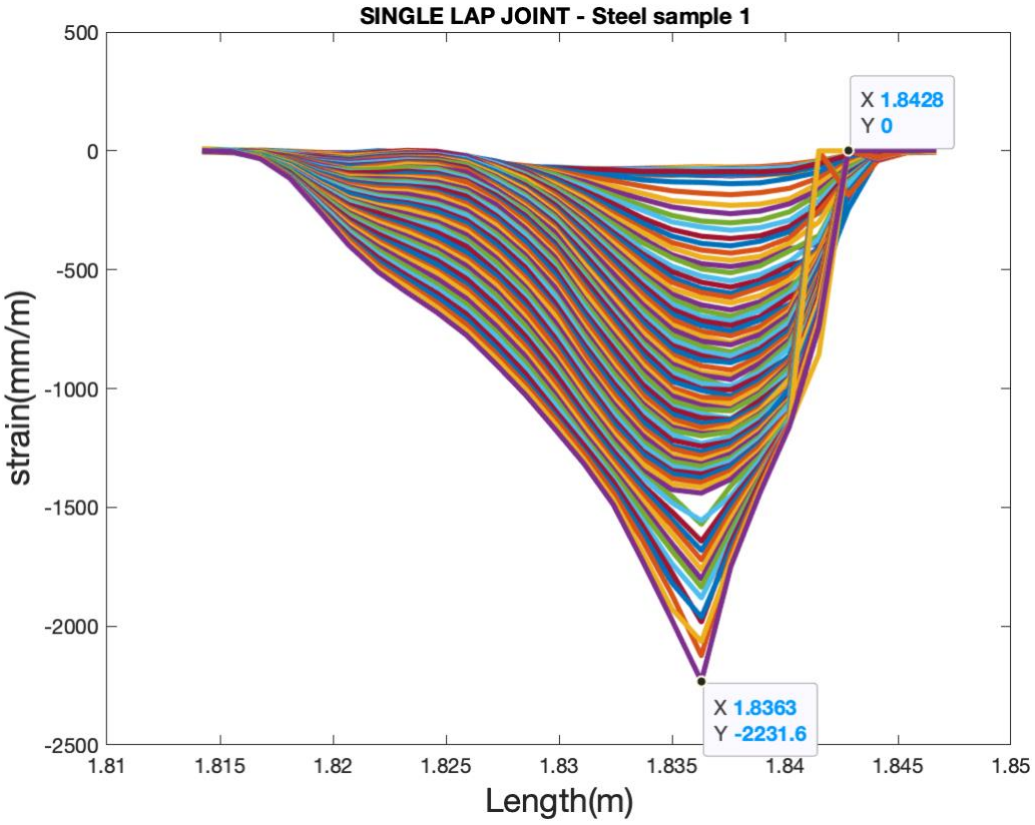

Figure 81. Strain vs Length steel sample 1

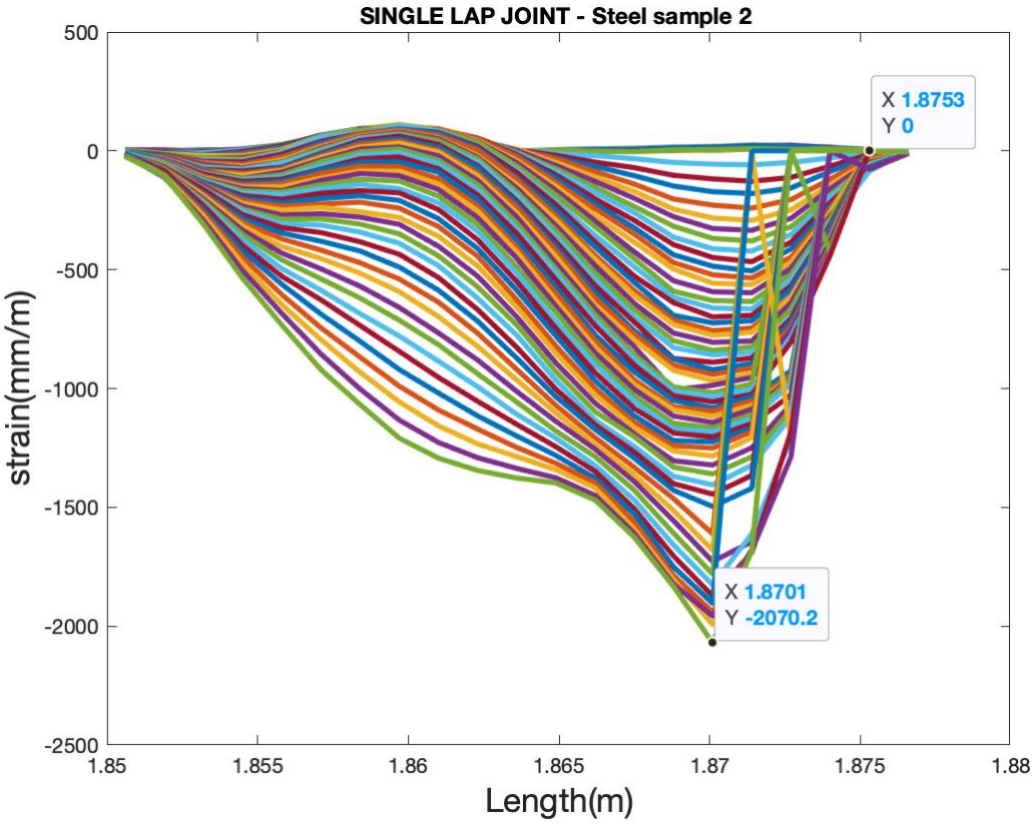

Figure 82. Strain vs length steel sample 2

To see the behaviour of different specimens with respect to each other, a comparison must be made. The strain results between the reference sample, sample 10, sample 11, and sample 15, are shown in, Figure 83. Before talking about the characteristic difference in the curves, the manufacturing difference between the specimens must be known. The width of all samples is kept constant. In the reference sample and sample 11, thickness varies; for the former, 4 layers of pre-preg have been used, while for the latter, 8 layers have been used. The overlap length between the two is kept at 20 mm. In between samples 10 and 15, the overlap length has been maintained at 10 mm, with the former having 8 layers in the adherend and the latter having 4 layers, respectively.

From the results thus obtained, it can be verified how these dimensional changes in adherend and the overlap length affect the peak strain values. To have a comparative behaviour among all these samples, monitoring the behaviour at a constant load will be done, and the strain values thus obtained will be seen. The magnitude of load will be taken keeping in mind the lowest value at which any one of these specimens fails or breaks down.

Figure 83 shows how, by varying the dimensional characteristics of the samples, the strain condition can be optimized. In sample 15, adherend thickness, as well as the overlap of the lap joint, are at a minimum, thus making it most prone to breakage, which is also reflected in the attached figure showing the maximum amount of strain in this sample. While the strain is decreasing when we analyse sample 11, having the maximum overlap length and thickness of adherend. The values in the other two samples lie between the maximum and minimum possible. Another point to be observed here is that the effect of overlap length is much greater than the effect created by adherend thickness.

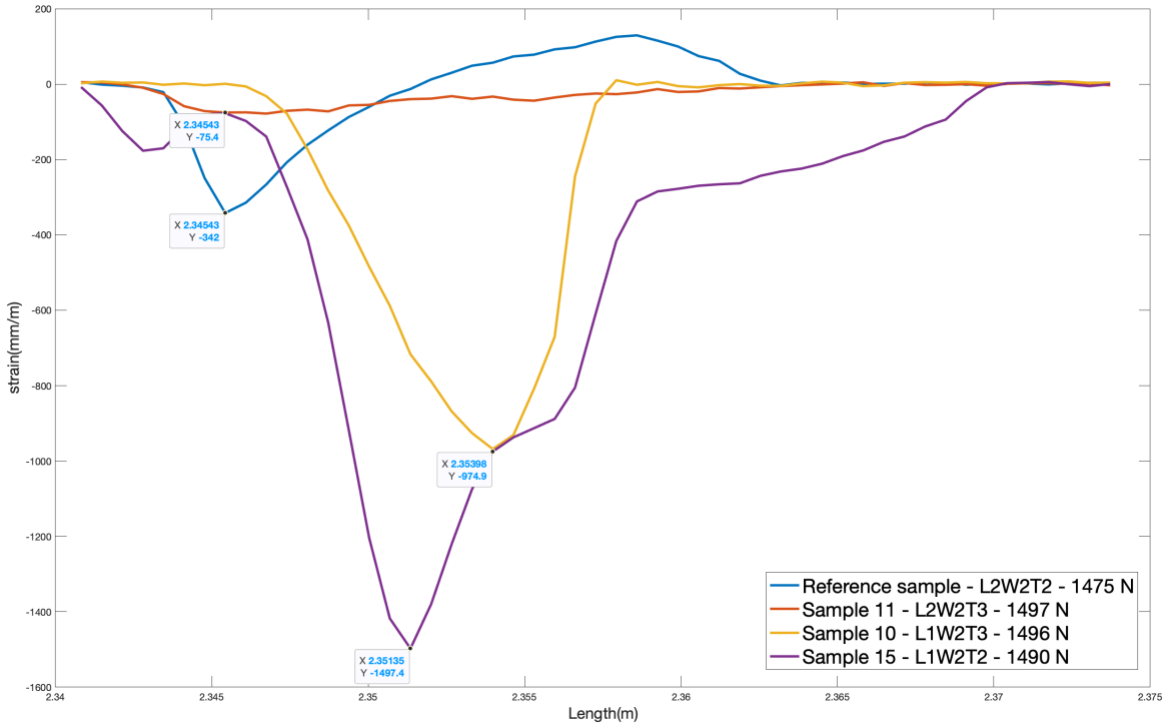

Figure 83. comparison showing the difference in the behaviour of different samples

Chapter 5: Conclusions

There has been immense learning from all the experimentation thus performed, beginning with joint formation. There needs to be an automated process for making the joints and pouring the adhesive. This will ensure even distribution and quality of the adhesive and decrease the amount of human error. Also, the automation will make sure that the edges of the joints are properly joined since the process of peeling is most prevalent on the edges. While working in the lab and making every effort to ensure the same thickness of adhesive between different specimens, it has never been possible to precisely manufacture the same thickness. But if automation is employed, this constraint can be overcome very easily.

The results that have been discussed above have also highlighted the importance of end tab thickness and how the moment is created due to the eccentricity thus encountered. Any experiments done in the future should always keep this point in mind to have proper results.

Additionally, the acquisition has solely been done using optical fibres. The basic handling of optical fibres is quite difficult, and to have a standard set of results for monitoring the structural health using fibres, the number of tests to be performed should be very high. This can provide the researchers with better insight into the capabilities of result analysis using optical fibres. The quality of fibres needs to be enhanced to a similar extent as that of pigtails. All the processes ranging from removing the outer jacket to cleaving, cleaning, and splicing are easier with pigtails, while it is the opposite in the case of the fibres used for acquisition. This obviously could be an additional cost, but that is what good research demands.

Apart from these constraints and precautions that have to be considered for obtaining useful results, the experimentation done shows how optical fibres act as a precise tool in structural health monitoring as compared to conventional elements like strain gauges. In the case of optical fibres, the results accurately point out the location of the maximum strain and breakage of the joint and also how the strain varies along the sought area. A modification could be made in terms of the alignment of the fibres. In the tests done above, analysis has only been performed in the longitudinal direction. The variation of mechanical properties in the transverse direction can also be checked by attaching the fibres in this way. This could provide information about the behaviour of the transverse edges as the load is transferred over the length of the joint.

References:

[1] E. Li, “Rayleigh scattering based distributed optical fibre sensing,” in *AOPC 2017: Fibre Optic Sensing and Optical Communications*, L. Wei, W. Zhang, D. Jiang, W. Wang, K. T. Grattan, Y. Liao, and Z.-S. Zhao, Eds., SPIE, Oct. 2017, p. 97. doi: 10.1117/12.2285293.

[2] J. Tong, F. J. Guild, S. L. Ogin, and P. A. Smith, “On matrix crack growth in quasi-isotropic laminates—I. Experimental investigation,” *Compos Sci Technol*, vol. 57, no. 11, pp. 1527–1535, Jan. 1997, doi: 10.1016/S0266-3538(97)00080-8.

[3] S. S. Kessler, S. M. Spearing, M. J. Atalla, C. E. S. Cesnik, and C. Soutis, “Damage detection in composite materials using frequency response methods,” *Compos B Eng*, vol. 33, no. 1, pp. 87–95, Jan. 2002, doi: 10.1016/S1359-8368(01)00050-6.

[4] C. L. Wilson, K. Lonkar, S. Roy, F. Kopsaftopoulos, and F.-K. Chang, “7.20 Structural Health Monitoring of Composites,” in *Comprehensive Composite Materials II*, Elsevier, 2018, pp. 382–407. doi: 10.1016/B978-0-12-803581-8.10039-6.

[5] M. Knight and D. Curliss, “Composite Materials,” in *Encyclopedia of Physical Science and Technology*, Elsevier, 2003, pp. 455–468. doi: 10.1016/B0-12-227410-5/00128-9.

[6] V. V. Vasiliev and E. V. Morozov, “Introduction,” in *Advanced Mechanics of Composite Materials*, Elsevier, 2013, pp. 1–27. doi: 10.1016/B978-0-08-098231-1.00001-7.

[7] M. K. Egbo, “A fundamental review on composite materials and some of their applications in biomedical engineering,” *Journal of King Saud University - Engineering Sciences*, vol. 33, no. 8, pp. 557–568, Dec. 2021, doi: 10.1016/j.jksues.2020.07.007.

[8] A. K. Sharma, R. Bhandari, A. Aherwar, and R. Rimašauskienė, “Matrix materials used in composites: A comprehensive study,” *Mater Today Proc*, vol. 21, pp. 1559–1562, 2020, doi: 10.1016/j.matpr.2019.11.086.

[9] Ageyeva, Sibikin, and Kovács, “A Review of Thermoplastic Resin Transfer Molding: Process Modeling and Simulation,” *Polymers (Basel)*, vol. 11, no. 10, p. 1555, Sep. 2019, doi: 10.3390/polym11101555.

[10] J. Liu, S. Wang, Y. Peng, J. Zhu, W. Zhao, and X. Liu, “Advances in sustainable thermosetting resins: From renewable feedstock to high performance and recyclability,” *Prog Polym Sci*, vol. 113, p. 101353, Feb. 2021, doi: 10.1016/j.progpolymsci.2020.101353.

[11] S. Laurenzi and M. Marchetti, “Advanced Composite Materials by Resin Transfer Molding for Aerospace Applications,” in *Composites and Their Properties*, InTech, 2012. doi: 10.5772/48172.

[12] H. Nguyen, W. Zatar, and H. Mutsuyoshi, “Mechanical properties of hybrid polymer composite,” in *Hybrid Polymer Composite Materials*, Elsevier, 2017, pp. 83–113. doi: 10.1016/B978-0-08-100787-7.00004-4.

[13] M. Ertekin, “Aramid fibres,” in *Fibre Technology for Fibre-Reinforced Composites*, Elsevier, 2017, pp. 153–167. doi: 10.1016/B978-0-08-101871-2.00007-2.

[14] “https://www.e-education.psu.edu/matse81/node/2214.”

[15] J. Gonzalo, W. J. Cantwell, and R. A., “Advantages of Low Energy Adhesion PP for Ballistics,” in *Thermoplastic Elastomers*, InTech, 2012. doi: 10.5772/34995.

[16] P. D. Mangalgiri, “Composite materials for aerospace applications,” *Bulletin of Materials Science*, vol. 22, no. 3, pp. 657–664, May 1999, doi: 10.1007/BF02749982.

[17] D. Blass, S. Kreling, and K. Dilger, “The impact of prepreg aging on its processability and the postcure mechanical properties of epoxy-based carbon-fibre reinforced plastics,” *Proceedings of the Institution of Mechanical Engineers, Part L: Journal of Materials: Design and Applications*, vol. 231, no. 1–2, pp. 62–72, Feb. 2017, doi: 10.1177/1464420716665413.

[18] K. C. Cole *et al.*, “Room-temperature aging of Narmco 5208 carbon-epoxy prepreg. Part II: Physical, mechanical, and nondestructive characterization,” *Polym Compos*, vol. 12, no. 3, pp. 203–212, Jun. 1991, doi: 10.1002/pc.750120311.

[19] K. Balasubramanian, M. T. H. Sultan, and N. Rajeswari, “Manufacturing techniques of composites for aerospace applications,” in *Sustainable Composites for Aerospace Applications*, Elsevier, 2018, pp. 55–67. doi: 10.1016/B978-0-08-102131-6.00004-9.

[20] X. Kornmann, M. Rees, Y. Thomann, A. Necola, M. Barbezat, and R. Thomann, “Epoxy-layered silicate nanocomposites as matrix in glass fibre-reinforced composites,” *Compos Sci Technol*, vol. 65, no. 14, pp. 2259–2268, Nov. 2005, doi: 10.1016/j.compscitech.2005.02.006.

[21] B. Middleton, “Composites: Manufacture and Application,” in *Design and Manufacture of Plastic Components for Multifunctionality*, Elsevier, 2016, pp. 53–101. doi: 10.1016/B978-0-323-34061-8.00003-X.

[22] “Manufacturing of fibre–polymer composite materials,” in *Introduction to Aerospace Materials*, Elsevier, 2012, pp. 303–337. doi: 10.1533/9780857095152.303.

[23] D. Dixit, R. Pal, G. Kapoor, and M. Stabenau, “Lightweight composite materials processing,” in *Lightweight Ballistic Composites*, Elsevier, 2016, pp. 157–216. doi: 10.1016/B978-0-08-100406-7.00006-4.

[24] J. P. Greene, “Injection Molding,” in *Automotive Plastics and Composites*, Elsevier, 2021, pp. 241–254. doi: 10.1016/B978-0-12-818008-2.00019-2.

[25] S. Lathabai, “Joining of aluminium and its alloys,” in *Fundamentals of Aluminium Metallurgy*, Elsevier, 2011, pp. 607–654. doi: 10.1533/9780857090256.3.607.

[26] “Introduction and Adhesion Theories,” in *Adhesives Technology Handbook*, Elsevier, 2009, pp. 1–19. doi: 10.1016/B978-0-8155-1533-3.50004-9.

[27] E. A. S. Marques, L. F. M. da Silva, M. D. Banea, and R. J. C. Carbas, “Adhesive Joints for Low- and High-Temperature Use: An Overview,” *J Adhes*, vol. 91, no. 7, pp. 556–585, Jul. 2015, doi: 10.1080/00218464.2014.943395.

[28] H. L. Groth, “Viscoelastic and viscoplastic stress analysis of adhesive joints,” *Int J Adhes Adhes*, vol. 10, no. 3, pp. 207–213, Jul. 1990, doi: 10.1016/0143-7496(90)90105-7.

[29] S. B. Kim, N. H. Yi, H. D. Phan, J. W. Nam, and J.-H. J. Kim, “Development of aqua epoxy for repair and strengthening of RC structural members in underwater,” *Constr Build Mater*, vol. 23, no. 9, pp. 3079–3086, Sep. 2009, doi: 10.1016/j.conbuildmat.2009.04.002.

[30] L. Loh and S. Marzi, “A Mixed-Mode Controlled DCB test on adhesive joints loaded in a combination of modes I and III,” *Procedia Structural Integrity*, vol. 13, pp. 1318–1323, 2018, doi: 10.1016/j.prostr.2018.12.277.

[31] J. Cui, S. Wang, S. Wang, S. Chen, and G. Li, “Strength and failure analysis of adhesive single-lap joints under shear loading: Effects of surface morphologies and overlap zone parameters,” *J Manuf Process*, vol. 56, pp. 238–247, Aug. 2020, doi: 10.1016/j.jmapro.2020.04.042.

[32] M. D. Aydin, A. Özel, and Ş. Temiz, “The effect of adherend thickness on the failure of adhesively-bonded single-lap joints,” *J Adhes Sci Technol*, vol. 19, no. 8, pp. 705–718, Jan. 2005, doi: 10.1163/1568561054890499.

[33] B. Wang, S. Zhong, T.-L. Lee, K. S. Fancey, and J. Mi, “Non-destructive testing and evaluation of composite materials/structures: A state-of-the-art review,” *Advances in Mechanical Engineering*, vol. 12, no. 4, p. 168781402091376, Apr. 2020, doi: 10.1177/1687814020913761.

[34] M. A. Hamstad, “A review: Acoustic emission, a tool for composite-materials studies,” *Exp Mech*, vol. 26, no. 1, pp. 7–13, Mar. 1986, doi: 10.1007/BF02319949.

[35] W. Broughton, “Testing the mechanical, thermal and chemical properties of adhesives for marine environments,” in *Adhesives in Marine Engineering*, Elsevier, 2012, pp. 99–154. doi: 10.1533/9780857096159.2.99.

[36] F. E. Oz, M. Mehdikhani, N. Ersoy, and S. V. Lomov, “In-situ imaging of inter- and intra-laminar damage in open-hole tension tests of carbon fibre-reinforced composites,” *Compos Struct*, vol. 244, p. 112302, Jul. 2020, doi: 10.1016/j.compstruct.2020.112302.

[37] G. R. Higson, “Recent advances in strain gauges,” *J Sci Instrum*, vol. 41, no. 7, pp. 405–414, Jul. 1964, doi: 10.1088/0950-7671/41/7/301.

[38] “https://www.michsci.com/what-is-a-strain-gauge/.”

[39] Y.-K. Zhu, G.-Y. Tian, R.-S. Lu, and H. Zhang, “A Review of Optical NDT Technologies,” *Sensors*, vol. 11, no. 8, pp. 7773–7798, Aug. 2011, doi: 10.3390/s110807773.

[40] S. Addanki, I. S. Amiri, and P. Yupapin, “Review of optical fibres-introduction and applications in fibre lasers,” *Results Phys*, vol. 10, pp. 743–750, Sep. 2018, doi: 10.1016/j.rinp.2018.07.028.

[41] A. Veber, Z. Lu, M. Vermillac, F. Pigeonneau, W. Blanc, and L. Petit, “Nano-Structured Optical Fibres Made of Glass-Ceramics, and Phase Separated and Metallic Particle-Containing Glasses,” *Fibres*, vol. 7, no. 12, p. 105, Nov. 2019, doi: 10.3390/fib7120105.

[42] I. Z. González, A. M. Valenzuela-Muñiz, G. Alonso-Nuñez, M. H. Farías, and Y. V. Gómez, “Influence of the Synthesis Parameters in Carbon Nanotubes Doped with Nitrogen for Oxygen Electroreduction,” *ECS Journal of Solid State Science and Technology*, vol. 6, no. 6, pp. M3135–M3139, Feb. 2017, doi: 10.1149/2.0251706jss.

[43] K. O. Hill and G. Meltz, “Fibre Bragg grating technology fundamentals and overview,” *Journal of Lightwave Technology*, vol. 15, no. 8, pp. 1263–1276, 1997, doi: 10.1109/50.618320.

[44] C. Campanella, A. Cuccovillo, C. Campanella, A. Yurt, and V. Passaro, “Fibre Bragg Grating Based Strain Sensors: Review of Technology and Applications,” *Sensors*, vol. 18, no. 9, p. 3115, Sep. 2018, doi: 10.3390/s18093115.

[45] A. Barrias, J. Casas, and S. Villalba, “Embedded Distributed Optical Fibre Sensors in Reinforced Concrete Structures—A Case Study,” *Sensors*, vol. 18, no. 4, p. 980, Mar. 2018, doi: 10.3390/s18040980.

[46] C. G. Berrocal, I. Fernandez, and R. Rempling, “Crack monitoring in reinforced concrete beams by distributed optical fibre sensors,” *Structure and Infrastructure Engineering*, vol. 17, no. 1, pp. 124–139, Jan. 2021, doi: 10.1080/15732479.2020.1731558.

[47] L. Chamoin, S. Farahbakhsh, and M. Poncelet, “An educational review on distributed optic fibre sensing based on Rayleigh backscattering for damage tracking and structural health monitoring,” *Meas Sci Technol*, vol. 33, no. 12, p. 124008, Dec. 2022, doi: 10.1088/1361-6501/ac9152.

[48] “https://it.rs-online.com/web/p/calibri/8412530?cm_mmc=IT-PLA-DS3A-_-google-_-CSS_IT_IT_Strumenti_di_misura_Whoop-_-(IT:Whoop!)+Calibri-_-8412530&matchtype=&aud-828197004210:pla-341201478706&gclid=Cj0KCQjw4s-kBhDqARIsAN-ipH00FPWH-yBLcJO5PAOcI2YoiJjFgVamUfVjCMryM7E2ieBl7AK5OUcaAoK2EALw_wcB&gclsrc=aw.ds.”

[49] “https://www.thorlabs.com/newgrouppage9.cfm?objectgroup_id=12731.”

[50] “https://www.optokon.com/optical-cables-and-fibres.”